Co-Diffusion of Social Contagions

DARTMOUTH

Ho-Chun Herbert Chang

Honors Thesis

Feng Fu, Advisor

Dartmouth College

April 24, 2018

Acknowledgement

Foremost, I'd like to thank Professor Feng Fu for his relentless enthusiasm, support, guidance, and always replying to my distress emails quickly. I'd like to thank Tommy Khoo for talking through results and the math involved, Jennifer Kuo for statistical help, Long Do for editorial advice from RWIT, Dr. David Cottrell for a last minute save with plotting, Jonathan Meng for coding suggestions, and Professor Sean Westwood for offering suggestions every step of the way. Lastly, I'd like to thank my family for their constant support from half-way around the world.

Abstract

Prior social contagion models consider the spread of either one contagion at a time on interdependent networks or multiple contagions on single layer networks and usually under assumptions of pure competition. We propose a new threshold model for the diffusion of multiple contagions. Individuals are placed on a periodic square lattice, and this population structure is later expanded to a multiplex with the addition of a random-regular-graph layer. On these population structures, we study the interface between two key aspects of the diffusion process: the level of synergy between two contagions, and the rate at which individuals become dormant after adoption. Monte Carlo simulations reveal lower synergy makes contagions more susceptible to percolation, especially those that diffuse on lattices. I show that within a band of synergy, contagions on lattices undergo bimodal or trimodal bifurcations if they are the slower diffusing contagion.

Word Count: 9970

Contents

List of Figures

Chapter 1

Introduction

The term "social contagion" implicitly captures two worlds: the world of social science and the world of epidemiology. Although the term was initially coined in 1895 by Gustave Le Bon [39] to describe undesirable collective behaviors in crowds, the definition has been stretched to encompass and explain types of collective behavior produced through social contact. This broad definition has led Contagion Theory's inclusion within many avenues of social science research [23], including marketing [58], innovation diffusion [28], medicine [57] and sociology [5].

In the same way that two contagions may influence each other's infectious paths, related innovations such as ideas, behaviors, products or technologies influence each others' diffusion. Prior social contagion models consider the spread of either one contagion at a time on interdependent networks or multiple contagions on single layer networks, usually under assumptions of pure competition. There is thus a desire to understand the diffusion of multiple social contagions under synergistic assumptions and to model the mechanisms for their concurrent, interfering spread. The thesis has three main objectives. First, drawing upon established models within epidemiology and pharmacology, I propose a model which quantifies the amount of synergy between two contagions. Secondly, I consider the effects of stochastic dormancy, or immunity,

towards similar contagions. This allows for the modeling of phenomenon that can be simultaneously cooperative and competitive. Lastly, I study the impact of network topology on the diffusion across short-range and long-range connections using random-regular-graphs.

In many ways, the term "social contagion" is an oxymoron. The word *contagion* by itself means a disease spread by contact, a process in which the active and passive agents do not get to decide whether they are infected or not. On the other hand, social sciences are built on the assumption that rational individuals have the agency to make decisions.

As a form of complex system modeling, agent-based modeling is based on the premise that simple assumptions about agents can lead to complex results, where these assumptions are simply characteristics of agents and need not imply agency. As we will discuss in Chapter 2, there are three scholars whose work this thesis draws from extensively, one of which is political scientist Robert Axelrod. In the second volume of the Handbook of Economics, he begins his chapter with his perspective on Agent-Based Modeling:

> This chapter describes some of my experiences with agent-based modeling (ABM) as a bridge between disciplines. I offer these experiences to provide concrete examples of how agent-based modeling can help overcome the somewhat arbitrary boundaries between disciplines. In graduate school, I took the micro-macro sequence designed to socialize the economic doctoral students into their discipline. I distinctly remember an occasion when the professor— a future Nobel Prize winner– was presenting a formal model of consumer behavior. A student remarked, But that's not how people behave. The professor replied simply, You're right, and without another word, turned back to the blackboard and continued his presentation of the model. We all got the idea.

The value of agent-based models is less so the transient observations in the simulation, but the converging and telling end-behaviors of complex system analyses.

Complex systems exhibit emergent phenomenon, and although the definition of emergence is still debated, a common definition is that the outcome cannot be simply predicted from its constituent parts. The framework used in mathematics to study this phenomenon today is encoded in graph theory. While the application of statistical physics to graphs was motivated by understanding percolation processes, scientists soon realized these could be applied to study other complex systems in economics, society and biology. This sub-field is generally known as network science.

A network reduces a system into individual entities called nodes which encapsulate characteristics and properties of the original system. Connections are represented by edges. One critique of any mathematical representation is that they are too reductive. Thus, a primary motivation in the field is how to enrich the model while with more information while keeping the tractable. An area of recent growth is with multiplex networks, or networks where the same set nodes are connected in multiple network layers and how this may be applied to Social Contagions [52].

This thesis is organized in the following way. Chapter 2 reviews the literature on diffusion in the network sciences with focus on academic fields and the researchers whom have made significant contribution. Chapter 3 develops necessary terminology, formulates the methodology for the two experiments and states the hypotheses in the context of the parameters. Chapter 4 analyzes the results of the experiments. Chapter 5 concludes the study, examines the weaknesses, discusses interpretation within certain areas of the social sciences, then proposes future avenues of investigation.

While I wrote this paper there was a debate about keeping terminology consistent. To this end there were a few challenges. Since I am borrowing epidemiological models, it is difficult to separate the vocabulary of biology such as infection, contagion and immunity from the discussion. At the same time, since I am modeling social behaviors,

the terms innovation and adoption seem more suitable. Thus, I default to contagion, and interchange adoption and infection as required within the context of discussion.

Chapter 2

Literature Review

This paper draws significantly from the seminal work of three scholars who work in different fields of research, yet produced important general diffusion frameworks. The first is communication theorist and sociologist Everett Rogers, who pioneered Innovation Diffusion in 1962. The second is aforementioned political scientist Robert Axelrod known for his application of agent-based modeling to study culture and cooperation. The third is Martin Nowak, who imports evolutionary dynamics and epidemiological modeling to study emergent social phenomenon. The contribution of these scholars come chronologically and the literature review is organized in the same fashion. I first give an overview of the historical development of innovation diffusion and give two examples of potential areas of application: cultural diffusion using Axelrod's model as an example. Information diffusion and technology innovation. I end with Nowak's epidemiological models for social contagions as the most contemporary example, which is the field this thesis offers contribution.

2.1 A Brief History of Innovation Diffusion

The diffusion of innovations address how new ideas and practices spread across a population. It has been studied since 1962, when Rogers published his work *Diffusion of Innovations* [51]. Following Rogers' initial publication, the 1960s saw a great deal of diffusion research which utilized adoption and economic data [55]. Now in its fifth edition, Roger's book has been cited more than 86,000 times, due to its wide applicability to information dynamics, economics [54], marketing, medicine and health care policy [21], and other fields of the social sciences. Many of these models have also introduced techniques and insight from the field of epidemiology [55]. Growth of computation and the network sciences in the 1990s spurred further interest in the aforementioned area, especially with the advent of large network technologies like the Internet.

The first quantitative model was the Bass Model (1969) [51], which uses the logistic function to estimate the rate of innovation [27]. The Bass Model served as a precursor to the spatial autocorrelation model, then the network autocorrelation model. More recently, researchers have adopted complex systems models to model the social phenomenon. This involves generating a graph, where each node represents an individual decision maker.

The classic Bass Diffusion Model exhibits behavior similar to the one-parameter logistic function, given as

$$y = \frac{1}{1 + e^{-b_1 t}} + b_0$$

with y the percentage of adopters, t as time, and b_1 the rate of adoption. A constant b_0 can be added to move the time scale. An extension allows feedback between adopters and imitators [4], given as:

$$y = b_0 + (b_1 - b_0)y_{t-1}b_1(Y_{t-1})^2 \tag{2.1}$$

This formulation has been useful in particular for disease spread from a central location [55]. In the social sciences, it has been useful for estimating the adoption from mass media advertisement. However, the Bass Model does not consider distance in any metric space; that is, it assumes perfect social mixing.

To mitigate this, an extension of Moran's model was proposed in 1956, where he considered the spatial distance between nodes. This is known as the Spatial Autocorrelation Model, expressed as follows:

$$I = \frac{N \sum_i^N \sum_j^N D_{ij}(y_i - \bar{y})(y_j - \bar{y})}{S \sum_i^N (y_i - \bar{y})^2}$$

D is the distance matrix (so the coordinates correspond to the weight), y denotes the adoption, and S is the sum of all distances. This allows Moran's I statistic to measure deviation of behavior from a nodes neighbor. For instance, the I statistic is high if connected nodes exhibit very different behaviors. However, this model simply gives a macroscopic indicator of diffusion, but does not show how the underlying network structure, or the types of individuals, that would influence the diffusion. Models that were built on networks and graphs were developed to address this deficiency.

2.1.1 Network Models of Innovation Diffusion

In network models, each node is its own decision maker who rationally decide whether they should adopt a certain behavior. Information cascades, or herding, is a phenomenon in which public information gleaned from those around an individual overpowers a node's private information and thus influence their decision making. These

effects are largely classified as informational network effects or direct benefit effects. Direct benefits exist when there is a benefit for copying the behavior of others. Any messaging online messenger service falls into this category, as the more of your friends adopt the communication technology the more likely you will be tempted to as well. Thus, the likelihood of a node's adoption, or infection, grows proportionally to his or her neighbor's adoption.

The second type falls under network effects. These are typically modeled with network coordination games, where each node plays with its neighbors and can be used to model competing contagions, for instance suppose n is a nodes neighbors, p the fraction that holds innovation A and $(1-p)$ the fraction that holds innovation B. The innovations have payoffs a and b respectively. Then the threshold is

$$p \geq \frac{b}{a+b} \tag{2.2}$$

Within the framework of coordination games, there have been well-established conclusions about what can prevent a cascade. Specifically, clusters are obstacles to cascades and clusters are the only inhibitor of cascades. This is shown in chapter 19 of *Networks, Crowds, and Markets: Reasoning about a Highly Connected World* [16]. Nodes with the highest potential to maximize spread are denoted as Influential Users [14]. Within scale free networks, clusters are also known as hubs, which are shown to be influential users [14]. Within single layered networks, seed selection have been well documented [31] using techniques such as K-Shell [32] and VoteRank [59]. Recent efforts focus on multi-layer networks as well using the same seed selection, in addition to Degree Centrality [17]. Seed selection is intimately tied with the topography of the network. Some models consider information as an

exchange or bartering activity between agents [12], and has been extended to a co-evolutionary experiment [44].

2.1.2 Culture Dissemination

In 1997, political scientist Robert Axelrod asked the question: if people tend to become more alike in their beliefs, attitudes, and behavior when they interact, why isn't it that all differences disappear? [3] In other words, why does cultural diversity persist even when homogeneous self-enforcement occurs within a group?

Axelrod defines culture as the set of features that are subject to social influence. His model is built on two assumptions. First, people are more likely to interact with people similar to them. Secondly, these interactions make them more similar. He gives the example of language, where an individual is more likely to interact with someone who speaks a similar language, and the interaction in turn will define future patterns of speech between them.

In his model, Axelrod assumes an $L \times L$ lattice, where each node represents a person with an embedded culture. Cultures have a set of features F, defined broadly with examples such as language, religion, and cuisine. Within each feature, there are q qualities or traits. Each individual x_i is defined by a state vector with the dimension of F, and each element takes on a value $\{0, 1, ..., q-1\}$.

His experiment is asynchronous— at each time step, a random node x_i is selected as the active agent, then one of its neighbors denoted as the passive agent is selected. They then interact based on probability $\frac{n}{F}$, where n corresponds to the number of features where they match. If the interaction is successful, then a random feature of the passive agent is copied over to the active agent.

He showed that if the number of features were greater than the number of states

for traits, then the system would converges to a monoculture. Stable homogeneous regions decrease with the number of features and increases with the possible states of a trait. Since then, researchers have extended his model in multiple directions. Klemm et al. complicates the model by considering the effects of noise [33], dimensionality [35][36], and topology [34]. Researchers have also addressed different interaction mechanisms. Centola et al [9] considers "network homophily", where the interaction mechanism changes concurrently with the actions of the nodes.

Because of the generality of agent-based models, Axelrod's model had spillover effects to other fields of the social sciences. Gonzalez-Avella et al. [20] consider the effect of mass media in processes of cultural diffusion, while Leydesdorff [40] investigates the evolution of competing technologies. The work of Klemm on topology in particular motivates this project, since we investigate long and short range relationships. This may find application in analyzing the interaction of culture across local connections and online networks like the world web.

2.1.3 Product and Technology Innovation

New products serve a purpose for both producers and consumers. Consumers mix and match existing product offerings to satisfy their needs, while producers profit from this supply and demand of innovation and differentiation. As a result, the field of product and technology innovation is one of the most widely studied fields of innovation diffusion. Langley et al. [37] note the role of social contagions in the process of innovation, then identify primary determinants that influence the diffusion process.

Chandrasekaran and Tellis notes competitive and complementary effects as an area of study [10]. The difference between competition and complementary action

becomes difficult to identify when competition may in fact help another innovation. A new brand can 1) increase the entire market potential due to its promotion and variety or 2) compete for the same market potential and slow down the diffusion. Guevara et al. (2007) [22] model the diffusion of two interacting products under the Generalized Bass diffusion Model (GBM) described in Equation 2.1, and more clearly define the different types of interactions between products. This was one of the first attempts to combine complementary and network effects under one GBM. They define two types of interactions. *Multi-product interactions* occur across product categories, such as hardware affecting software diffusion, while *network externalities* occur within a category, such as the user base.

Diffusion models that consider multi-product effects have received less attention. Bayus (2000) *Growth Models for Multiproduct Interactions: Current Status and New Directions* was one of the first studies to distinguish multiple product interactions beyond simple technological substitution and between successful generations. They partition models into two categories. The first include single-innovation diffusion models that parametrize the effects of multi-product interactions [50] [24]. The second considers generations of products and their succession dynamics [46].

Peres, Muller and Mahajan give a review of contemporary research directions [49]. They explicitly define innovation diffusion as "the process of the market penetration of new products and services that is driven by social influences, which include all interdependencies among consumers that affect various market players with or without their explicit knowledge." This is motivated by a movement towards higher degrees of interaction during the diffusion process, but contemporary research primarily focuses on competitive interactions. Literature that ties the general mathematical models described in Chapter 3 show that network externalities affect the rate of adoption, as

well as lead to adoption of an inferior technology if the network effects are sufficiently high [18] [2]. A standard method these papers use to fit their model to empirical data, such as IT to computer adoption [22].

General Purpose Technologies (GPTs) are an important concept in considering the co-diffusion of innovations. GPTs denote technologies that have impact across sectors and spillover effects as network externalities with economic benefits. Economists Lipsey and Carlaw have defined 24 GPTs, classified with four criteria [42]:

1. Is a single, recognizable generic technology
2. Initially has much scope for improvement but comes to be widely used across the economy
3. Has many different uses
4. Creates many spillover effects

GPTs often serve as pre-requisites for new eras of productivity, with Artificial Intelligence being the most recent one. Jovanovic and Rousseau studied the diffusion of electricity and information technologies, as well as their similarities [29]. Contemporary efforts on the front of co-diffusion include Lazzati [38], who tackles the question of maximizing technology with a fixed set of technologies to distribute.

with the eminent arrival of the next GPT revolution with artificial intelligence, finding means to predict and benchmark the diffusion of related innovations within artificial intelligence or relative to the GPT itself is both useful and timely. For instance, technology adoption manifests through both observing physical neighbors and online through the contemporary influence of social media.

2.2 Epidemiological Modeling of Social Contagions

Within the epidemiology literature, multiple infections have been extensively studied and the increased likelihood of becoming infected conditional on a first due to weakened immune systems is well-documented. Super-infection denotes the process of infecting an already infected individual with a second, typically more severe virus. Examples include HIV and Herpex Simplex Virus type 2.

Nowak and May were one of the first to model super-infection, where they assumed only the strongest virus is active and thus the only one that spreads [48]. Shortly afterwards, they modeled co-infection where multiple viruses are active [45]. Super-infection was then shown to be a limit of co-infection, and also gives the parameters in which multiple viruses can coexist. Similar to technology diffusion studies, competition is also modeled using cross-immunity in the context of a network [56].

Contemporary research can be divided into ones that focus on the network structure and ones that focus on the diffusion mechanism. Starting with network structure, Shu et al. [52] presents the dynamics of social contagions on two interdependent two-dimensional lattices. They give examples of nodes in communication networks which are spatially embedded. Li et al. [41] has a similar set-up to study the spread of epidemics, but in two experiments they first pair two interconnected lattices, then pair two Erdos-Renyi networks. In contrast, this thesis considers one lattice and one random-regular-graph, and thus investigates the interplay of spatial and long-range graphs. Aleta and Moreno [1] give a comprehensive review of how multilayer networks are used various contexts, including diffusion and percolation, and how this is applied to ecology, biology, transportation, economics, game theory, and transportation.

In regards to the diffusion mechanism, one common paradigm is the susceptible-infected-susceptible (SIS) model. In the basic SIS model, individuals transition be-

tween states of susceptibility and infection, where recovered individuals are once more susceptible. In other words, recovery from disease confer no immunity. Hill et al. [26] characterizes an SISa model, in which they distinguish between spontaneous and contagious infection. Hill et al. [25] has also modeled emotion as an infectious disease in large scale networks using the same SISa model. Dodds and Watts [15] provide a generalized model for social and biological contagions also using the SIS model, and identify three basic classes of contagion models which they call *epidemic threshold*, *vanishing critical mass*, and *critical mass*, and how one may interpret results for prevention or facilitation based on these cases. While the examples above occur on single layer networks, Liu et al. [43] has modeled epidemic spread on interconnected small-world networks, where neighbors of a node are likely to be neighbors of other nodes. Precisely, the typical distance L between two nodes chosen at random will grow proportionally to $\log N$ with N the number of nodes.

In regards to multiple infections, Chen et al. [11] proposes a model built on intrinsic properties of cooperative contagions A and B. Their model is also based on the SIS model where host individuals are in two possible states: susceptible (S) or infected(I). Susceptibles are equivalent to naive agents and can be infected by either A or B, each associated with a cooperativity coefficient ξ_A and ξ_B respectively to capture their mutual influence.

The Susceptible-Infection-Recovered (SIR) model in contrast confers a removed or recovered status to individuals, who are no longer susceptible to disease [47]. Immunity is a parameter that has analogous application in social systems, such as resistance to rumors-spreading or belief-change.

In sum, my thesis provides three specific contributions. First, it considers a new permutation of multiplex layer where a spatial network is coupled with one that

allows long range connections. Second, it considers multiple contagion diffusion on interdependent networks. Third, it considers the effect of immunity within the context of social contagion diffusion.

Chapter 3

Materials and Methods

3.1 Definitions and Terminology

Networks are represented mathematically by graphs. A graph is notated as $G = (V, E)$, where V is a set of nodes called vertices and E is the set of links called edges. Every element in E is represented by the Cartesian Product of two vertices $V \times V = (v_i, v_j)$, since each link must have two endpoints. If (v_i, v_j) is ordered, the graph is said to be directed; if order is irrelevant such that $(v_i, v_j) = (v_j, v_i)$ then the graph is undirected.

A multiplex network is a network where the same set of nodes are represented in every layer, although the interactions and links between the nodes may be different. Indeed, the motivation for this thesis is to study the diffusion of different contagions under different graph structures. For instance, a person's physical neighbors exist on a different network than the person's online presence, since the first graph is constrained physically while the latter allows for long-range links.

3.2 The General Algorithm

It is tempting when working with mathematical models to introduce parameters that may be only meaningful within the circle of applied mathematics. Thus, the variables and framework included are justified with fundamental and well-established facts from social contagion theory and innovation diffusion theory, and utilize analogous aspects of existing epidemiological models.

Without loss of generality, assume that we have two contagions: Contagion A and Contagion B. Every node in the experiment must take on one of four states: $\emptyset$, A, B, and AB, which correspond to uninfected/naive individuals, adopters of Contagion A, adopters of Contagion B, and adopters of both Contagion A and B. Diffusion denotes the spread of a contagion across a network, which influences the particular status of a node. Furthermore, each node is either active or dormant, represented by the Boolean 1 or 0 respectively. The status for each node is expressed as the tuple $(\text{State}, \text{Activity})$. For instance, an active node infected with A would be represented by $(A, 1)$. Each iteration of the simulation can be summarized as:

- Initialize a graph
- Seed Contagion A and Contagion B
- Diffuse graph by one time-step
- Count the nodes for the Uninfected, Contagion A, Contagion B, and both A and B
- Repeat from Step 3 until the last time-step

The raw output for each experiment are four time series. The general algorithm is described in Algorithm 1:

α-list = list of alpha values
τ_A-list = list of τ_A values
τ_B-list = list of τ_B values, with the constraint that $\tau_B < \tau_A$
ParameterList = list of tuples containing (α, τ_A, τ_B)
for *ParameterSet in ParameterList* **do**
  for *Number of Iterations* **do**
    Create graph G
    Randomly seed one of Contagion A and Contagion B into the nodes, non-overlapping
    Set a random threshold for each node
    for *All time-steps* **do**
      Diffuse the Contagions using a multivariate probability distribution
      Deactivate nodes based on probabilities τ_A and τ_B
      Count the total number of Uninfected, Contagion A, Contagion B, and Both Contagions
    end
    Save the individual time-series
  end
  Average time-series for each of the four categories
end

Algorithm 1: Algorithm for simulating network diffusion

The full list of parameters can be found in Section 3.5. As this is computationally very extensive, the for-loops were parallelized. Simulations were parallelized across parameters and run using a cluster of 600 CPUs. The sections below walk through the specific details of each step in Algorithm 1.

3.3 Initializing the Graph

Simulations were run on two types of graphs, all of which are undirected. The first simulation is defined on a periodic square lattice with length $L = 80$, which totals 6400 nodes. This means the degree of each node is 4 and neighbors are all spatially related.

The second simulation is a multilayer network diffusion experiment. One layer is

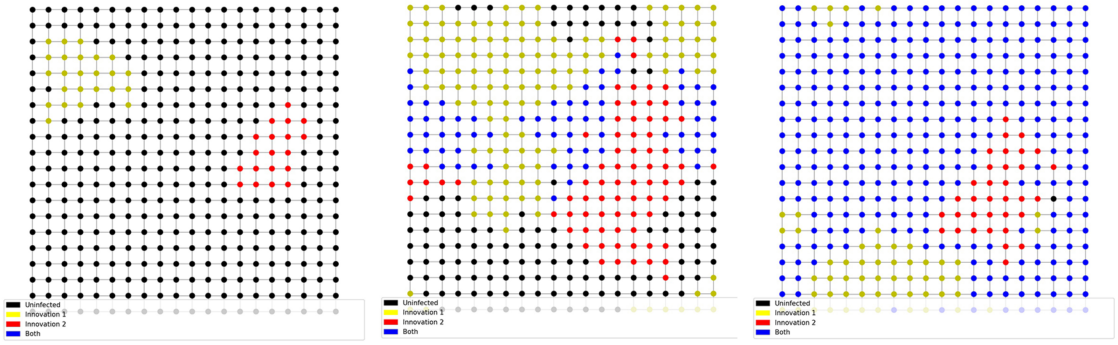

Figure 3.1: Single-Layer Lattice Diffusion
Innovation A (yellow) and Innovation B (red) spread to their von Neumann neighbors, then overlap with increased time steps as shown in blue.

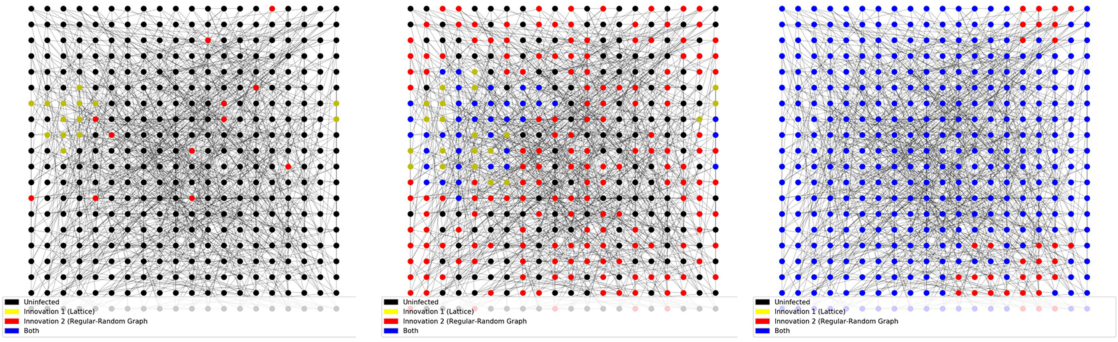

Figure 3.2: Multiplex Diffusion
Innovation A (yellow) spreads across the periodic lattice. Innovation B (red) spreads on the random-regular-graph, which show up as isolated points on the lattice. The dark, faded blotches are the edges of the random-regular-graph.

the periodic square lattice, the second is a random-regular-graphs with degree four. This is done to limit the effects of hubs, since every node has the same degree. The distinction between the periodic square lattice and the random-regular-graph is that now long-range edges are allowed, so I can compare the diffusion results of long-range connections versus the spatially localized. As I will discuss in Section 3.4.2, the threshold for A is determined by the neighbors on the lattice graph while the

threshold for B is determined from the random-regular-graph. Figure 3.2 illustrates the diffusion process.

From these nodes, one node is randomly selected, then seeded with Contagion A. Another one is seeded with Contagion B, with no repetition.

3.4 Adoption Probability Kernel

Section 2 of the literature review describes the assumptions within innovation diffusion, one of the main ones being that we can model the diffusion using a logistic function. The Hill Function is the log-transform of the logistic function and is useful in modeling density-dependent growth since it takes density as a direct parameter. It has roots in biochemistry is was used to measure the rate of reaction between reactant concentration and substrate density. The Hill function is given as:

$$f(X) = \frac{[X]^{\alpha}}{[X]^{\alpha} + K^{\alpha}} \tag{3.1}$$

where $[X]$ is the density of X, K denotes the time-step that is half-way to full saturation, and α is a shape parameter that determines how steep the slope of the function is. In other words, increasing K corresponds to shift right, although its shape becomes less steep as well. The ratio between α and K influences the steepness. Researchers in pharmacology noticed that the effect of drugs on killing cells and bacteria could be modeled similarly, and then extended the model to capture the effects of drug interaction.

3.4.1 The BLISS and Loewe Additivity

Traditional Chinese medicines typically use mixtures of herbs to maximize the potency during the healing process. This notion has not escaped the contemporary field of pharmacology, and the last century has seen the increased use of drug combinations.

Since studies have shown that for social contagions, density matters more than numbers, existing models within the pharmacology literature prove suitable for the co-diffusion model. Theoretical research within the field quantify the concepts of synergy and antagonism, which go beyond the simple additive effect from using drugs individually.

The Bliss Independence Model [19] assumes that drug effects are outcomes of probabilistic processes, but each contribute to a common result. This model is filed under a effect-based strategies, which compare the effects resulting from both drugs versus individual components. In this case, effect refers to the efficacy of killing bacteria or certain types of cells.

The second strategy for analyzing the efficacy of two drugs considers what concentration of each produces the same response [19]. The mathematical framework known as Loewe Additivity utilizes this Dose Equivalence Principle (DEP) to formalize definitions of synergy, additivism, and antagonism. The DEP states that dose a is equivalent to b_a where [19]

$$E(a+b) = E(a+a_b) = E(b_a+b)$$

For the sake of discussion in this section, suppose we have drugs A and B, each

administered at doses a and b respectively. This yields the combination index

$$CI = \frac{a}{A} + \frac{b}{B}$$

. For $CI < 1$, this indicates that that the combined amount of the two drugs required to produce a certain effect is less than the amount required when they are used individually. In other words, the combination is more effective and thus they act synergistically. Similarly, $CI > 1$ indicates that the combination of a and b produces a worse effect and is antagonistic.

Dose effects typically follow the logistic shape of the Hill equation defined as:

$$E = E_{max} \frac{a^{\alpha}}{k_a + a^{\alpha}}$$

where a denotes the concentration of A, E_{max} denotes the maximum effect or the ceiling, and k is the inflection point of the curve. What this model gives us is a general framework that is grounded in similar empirical observations in the fields of innovation diffusion and drug effectiveness. Instead of considering how two drugs work together to kill cells, I consider how innovations spread concurrently.

3.4.2 Probability Kernel for the Threshold

We treat an increase of the number of neighbors as a **threshold lowering effect**. As with the typical threshold model, each node is assigned a threshold μ_k, where:

$$\mu_i \in (0, 1) \qquad \text{where } i \text{ is the coordinate of each unique node}$$

A simple threshold is given in Equation 2.2, but it is insufficient to characterize the logistic shape of diffusion in different network settings. Here we develop thresholds under the assumption that each innovation individually diffuses according to the shape of a Hill Function. We have assumed, without loss of generality, that we have two products A and B. Assume that inclusive adoption is possible. We also assume that only one innovation can be adopted per time-step. Then there are two possible paths of adopting both A and B. Let i denote a node.

$$\begin{aligned} i(\text{Naive}) &\rightarrow i(A) \rightarrow i(AB) \\ i(\text{Naive}) &\rightarrow i(B) \rightarrow i(AB) \end{aligned} \tag{3.2}$$

or simply put, the naive/uninfected individual must adopt A first or B first. This is known as inclusive adoption. Exclusive adoption denotes the case where the state $\phi_i(AB)$ is not possible. Next, we denote an indicator function for the status where:

$$S_A(i) = \begin{cases} 1 & \text{if } i \text{ adopts A} \\ 0 & \text{if otherwise} \end{cases} \qquad S_B(i) = \begin{cases} 1 & \text{if } i \text{ adopts B} \\ 0 & \text{if otherwise} \end{cases}$$

Thus, the inclusive adoption probability of any state can be expressed using this general formula:

$$P(i) = \frac{\Big(1 - S_A(i)\Big)\Big(\frac{[A]}{K_A}\Big)^{\alpha} + \Big(1 - S_B(i)\Big)\Big(\frac{[B]}{K_B}\Big)^{\alpha}}{1 + \Big(1 - S_A(i)\Big)\Big(\frac{[A]}{K_A}\Big)^{\alpha} + \Big(1 - S_B(i)\Big)\Big(\frac{[B]}{K_B}\Big)^{\alpha}} \tag{3.3}$$

where K_A and K_B controls the attractiveness of each social contagion. The smaller the value, the more attractive it is to the population since it controls for the time step of the inflection point. $[A]$ denotes the density of neighbor nodes that have already

adopted innovation A. Specifically, let T be the total number of neighbors, then:

$$[A] = \frac{\text{No. of A}}{T} \tag{3.4}$$

The assumption is that α and K are known and can be fit based on past data. For the purpose of this study we assume $K_A = K_B = 2.0$, where the choice of this parameter suits the simulation time scale. To clarify Equation 3.3, we break down the sub-cases. For the naive individual i the values of $S_A(i)$ and $S_B(i)$ are both zero. Hence the adoption rate of either A or B can be characterized by:

$$P(i \leftarrow A \text{ or } B) = \frac{\left(\frac{[A]}{K_A}\right)^{\alpha} + \left(\frac{[B]}{K_B}\right)^{\alpha}}{1 + \left(\frac{[A]}{K_A}\right)^{\alpha} + \left(\frac{[B]}{K_B}\right)^{\alpha}} \tag{3.5}$$

The node is first activated with this probability. Then it will choose one of A and B based on their relative proportions. That is,

$$\Pr(i \leftarrow A) = \frac{\left(\frac{[A]}{K_A}\right)^{\alpha}}{\left(\frac{[A]}{K_A}\right)^{\alpha} + \left(\frac{[B]}{K_B}\right)^{\alpha}} \qquad \Pr(i \leftarrow B) = \frac{\left(\frac{[B]}{K_B}\right)^{\alpha}}{\left(\frac{[A]}{K_A}\right)^{\alpha} + \left(\frac{[B]}{K_B}\right)^{\alpha}} \tag{3.6}$$

Here, the notation $\Pr(i \leftarrow A)$ denotes the probability of node i adopting Contagion A, and it is the analogous case for B. The adoption probability is shown as a surface in Figure 3.3. In lieu of Loewe Additivity described in Section 3.4.1, these surfaces indicate the different relationships of synergy and antagonism. When $0 < \alpha < 1.0$, the curve is concave downwards, which indicates that the effect of their sum is more than their parts and thus synergistic. When $\alpha > 1.0$ as with the case in the bottom right, the relationship is concave upwards which indicates antagonism. This corresponds to the formulation given in the isobologram analysis of [19].

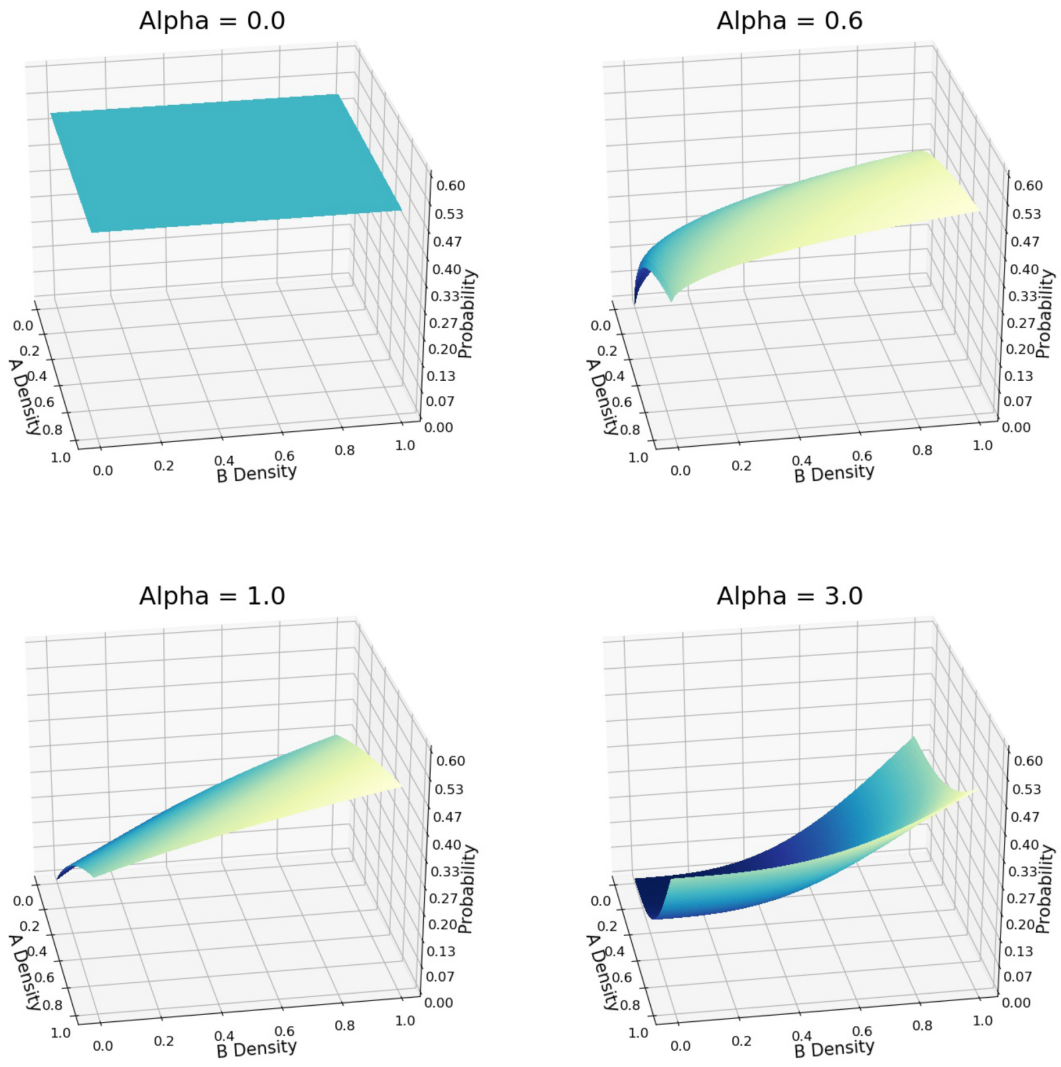

Figure 3.3: Adoption Probability Kernel
The surface of Equation 3.5, which describes the probability of adopting either A or B, depending on the densities of A and B. Here we assume $K_A = K_B = 2.0$.

Now without loss of generality suppose i has already adopted A. Then the prob-

ability of adopting B is given by

$$\frac{\left(\frac{[B]}{K_B}\right)^{\alpha}}{1+\left(\frac{[B]}{K_B}\right)^{\alpha}}$$

The case for adopting A after first adopting B is analogous.

In the experiment we set the thresholds as a function of this adoption probability. The threshold μ_i is given in Equation 3.7:

$$\mu_i = 1 - P(i \leftarrow A) \tag{3.7}$$

Then at every time step a random number is chosen between 0 and 1 to determine the probability of adoption. Ultimately, the formulation shown in Equation 3.3 captures synergistic diffusion as the initial adoption depends on both densities.

3.4.3 Exclusive Adoption

While not explicitly studied in this paper, exclusive adoption is a useful contrast to our case above. The adoption pathways can be represented as:

$$\begin{aligned} i(\text{Naive}) &\rightarrow i(A) \rightarrow \text{Immunity against B} \\ i(\text{Naive}) &\rightarrow i(B) \rightarrow \text{Immunity against A} \end{aligned} \tag{3.8}$$

The expression for adopting any of the contagions is thus:

$$P(i \leftarrow A \text{ or } B) = \Big(1 - S_A(i)\Big)\Big(1 - S_B(i)\Big)\frac{\left(\frac{[A]}{K_A}\right)^{\alpha} + \left(\frac{[B]}{K_B}\right)^{\alpha}}{1+\left(\frac{[A]}{K_A}\right)^{\alpha} + \left(\frac{[B]}{K_B}\right)^{\alpha}} \tag{3.9}$$

It then chooses A or B with the coin-flip expressed in Equation 3.6.

3.4.4 Stochastic Dormancy

The prior two parameters α and K model the shape of diffusion, and thus they only influences the timescale of diffusion. As time approaches infinity, the diffusion process will always diffuse to the maximal value. This is not the case in reality, as the penetration depth is usually a subset. We model this by introducing stochastic dormancy to every node on the graph, such that nodes are not active in perpetuity.

To do this, we attach a constant τ_A and τ_B to contagions A and B respectively. τ_A denotes the probability that a node infected with A will become dormant at any given time step. When a node is considering adoption, if a neighbor is dormant then that neighbor is discounted from the numerator of the density, and is thus not included in the threshold lowering effect. To be numerically precise,

$$[A] = \frac{\text{No. of Active A}}{T} \tag{3.10}$$

The same holds for Contagion B. Another way of interpreting τ is that τ_A represents the average proportion of nodes infected by A that will switch off at each time-step. For nodes infected with both A and B, the τ_{AB} value is simply the arithmetic average; different conditions for convexity is another line of inquiry. The expression is given as:

$$\tau_{AB} = \frac{\tau_A + \tau_B}{2}$$

It is important to distinguish between *immunity* and *dormancy*. In epidemiology both immunity and recovery imply two things— a recovered individual can no longer be infected nor can it infect other nodes. For the purpose of studying social contagions we relax the first condition. In other words, while inactive individuals no longer affect other nodes, they themselves can still be infected by another contagion. Thus, they

do not gain immunity from being infected, but they do less to help the contagion spread. We make a basic assumption that neighbors have to make a decision and play an active role in the diffusion process.

3.5 Experimental and Measured Variables

For each node at each time step, its activity and status (denoted as Uninfected, A, B, or AB) is updated. The largest constraint on computational resources was memory, so we updated via a dictionary approach rather than saving a copy of the graph. Monte Carlo simulations were performed with 100 iterations per parameter set. The following table summarizes the experimental parameters:

Table 3.1: Exogenous Variables

Parameter	**Quantity**
Number of Nodes	6400
Total Timesteps	700
Number of Initial Seeds	1
Iterations per Parameter Set	100

Table 3.2: Independent Variables

Parameter	**Quantity**
α range	0.0 to 1.3
τ range for Lattice	0.0 to 1.8
τ Range for Multiplex	0.0 to 1.0

The primary variable of interest is the depth of diffusion. This is taken as the equilibrium value at the end of diffusion, found by taking the diffusion depth of the final 20% of periods. Secondly, the rate is defined by the time-step that corresponds to the inflection point, or exactly one half of the ceiling.

3.5.1 Experiment 1: Diffusion on the Single Layer Lattice

Experiment 1 is defined on a single layer, 80×80 periodic square lattice. Since the diffusion of contagion A and Contagion B is parametrized the same way, we can simple perform half the necessary grid search as the results should be symmetric.

3.5.2 Experiment 2: Diffusion on the Multiplex Network

The diffusion on multiplex networks follows the same processes as Sections 3.4.2 and 3.4.4, however, the network topology is now a factor in counting the neighbors. As previously described, Contagion A diffuses on a 80×80 periodic square lattice and Contagion B diffuses on a random-regular-graph with degree 4. Precisely, for each node considering the adoption of Contagion A, only the active neighbors on the lattice graph are considered; for the adoption of Contagion B, only active neighbors on the random-regular-graph is considered.

3.6 Theoretical Derivation

3.6.1 Co-Diffusion in Well-Mixed Populations

We derive an expression for the rate of co-diffusion in a well-mixed population with degree κ. We define the adoption rate of Contagion j as ϕ_j and we denote the adoption of A and B as AB. Thus explicitly:

$$\begin{cases} \phi_A & := \text{Adoption Rate of A} \\ \phi_B & := \text{Adoption Rate of B} \\ \phi_{AB} & := \text{Adoption Rate of A and B} \end{cases}$$

Next, define the proportion of each type as x_A, x_B, x_{AB}, $x_\emptyset$, and x_R, where the subscript $\emptyset$ denotes naive individuals and R denotes dormant individuals. Note that x_A, x_B and x_{AB} only include naive individuals that— nodes that are dormant. Now we state our mean-field equations:

$$\begin{cases} 1 & = x_A + x_B + x_{AB} + x_\emptyset + x_R \\ \dot{x}_A & = x_\emptyset \phi_A(x_A, x_B) - \tau_A x_A \\ \dot{x}_B & = x_\emptyset \phi_B(x_A, x_B) - \tau_B x_B \\ \dot{x}_{AB} & = x_A \phi_{AB}(x_A, x_B) + x_B \phi_{AB}(x_A, x_B) - \tau_{AB} x_{AB} \\ \dot{x}_R & = \tau_A x_A + \tau_B x_B + \tau_{AB} x_{AB} \end{cases} \tag{3.11}$$

In layman language, the first equation states that there are five groups whose proportions sum to on. Equations two through five denote the rate of change for each respective sub-group. The rate of change for A, denoted $\dot{x}_A$ is equal to the adoption rate of A multiplied by the total proportion of A, subtracted by $\tau_A x_A$, the total number of nodes that go dormant. It is the same case for Contagion B and both. The last equation describes the nodes that go dormant, which is the sum of all the τ's multiplied by their respective sub-groups.

Chapter 4

Results

4.1 Lattice Diffusion

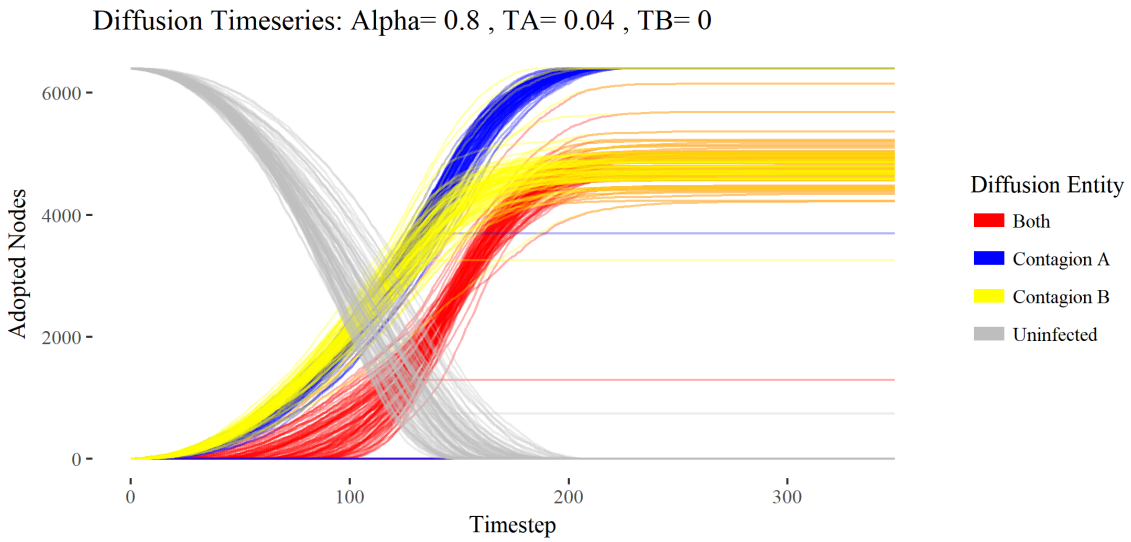

Figure 4.1: Time-Series of One Parameter Set
The diffusion curves of Contagion A (blue), Contagion B (yellow), Both A and B (red), and Uninfected nodes (grey). Parameters are set with $\alpha = 0.8$, $\tau_A = 0.04$, and $\tau_B = 0.00$.

The basic output of each experiment is shown in Figure 4.1. Contagion A shown

in blue diffuses completely, whereas Contagion B shown in yellow diffuses partially. Using the methods described in Chapter 3, the penetration depth and the inflection point was extracted as our primary variables of measurement. I use the term *ceiling* in lieu of penetration depth. I consider the inflection point as a proxy for rate, as it represents the time-step where the diffusion curve attains exactly half of its ceiling. If this point is pushed right, this indicates diffusion takes a longer time and thus the rate is lower. However, because it is a function of the ceiling, the inflection point decreases when the ceiling decreases so the use of rate is only useful for fixed-ceiling comparisons.

Thus, the most important variable is the ceiling. Since the parametrization of Contagion A and B are the equivalent, by symmetry we only need to analyze the results for the statuses A and AB. The mean results are summarized using the heat-map in Figure 4.2. The dark striations between the colored blocks are artifacts of conserving computational resources used in the grid-search. When $\alpha = 0$ the ceiling is maximal regardless of the value of τ_A and τ_B. This can be seen in Figure 3.3. The diffusion probability is a high 50% and as a result both contagions diffuses rapidly.

As we increase α the ceiling diminishes clearly, except for the case when $\tau_A = \tau_B = 0$, in which the ceiling remains uniformly red. This can be observed in the bottom left corner of all nine values of α. We can thus conclude that the value of τ influences the ceiling significantly. Now, consider the bottom row of the facet grid where α is equal to 1.1, 1.2, and 1.3. Indeed, as τ_A increases there is a clear gradient between from red to blue spanning left to right that indicates a diminishing ceiling. The gradient effect is particularly evident when we fix $\tau_B = 0$. In contrast, τ_B only produces an effect when it jumps from 0 to 0.02. This is actually a very deep result that requires more analysis by studying the standard deviation of diffusion and the

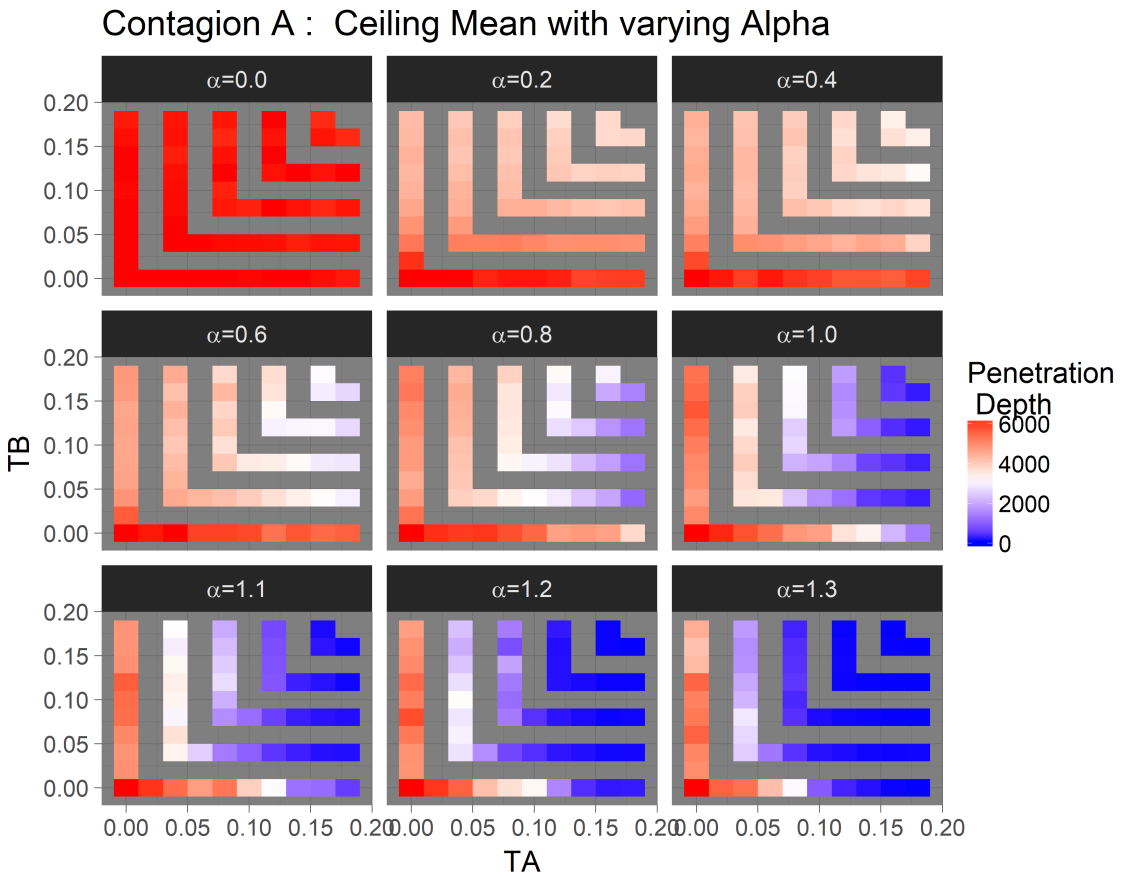

Figure 4.2: Ceiling Mean Heat-Map of Contagion A
Maximal penetration at 6,400 nodes is represented in red, while no penetration is represented in blue. Each graph denotes a different value of α.

actual time-series itself.

Additionally, the gradient effect is much less pronounced at low values of α. This suggests τ is sensitive to the rate of diffusion. To explain this we need to first refer to Figure 4.3. There, it is clear that α slows the rate of diffusion as the time-step where the curves reach the inflection points increases. The effect of α on timescale is by construction. As shown in Figure 3.3, increasing α causes a diminished probability of adoption, which, in the case where $\tau_A = \tau_B = 0$, that means it takes longer for the contagions to diffuse to the maximal value of 6,400 nodes. In other words, the longer

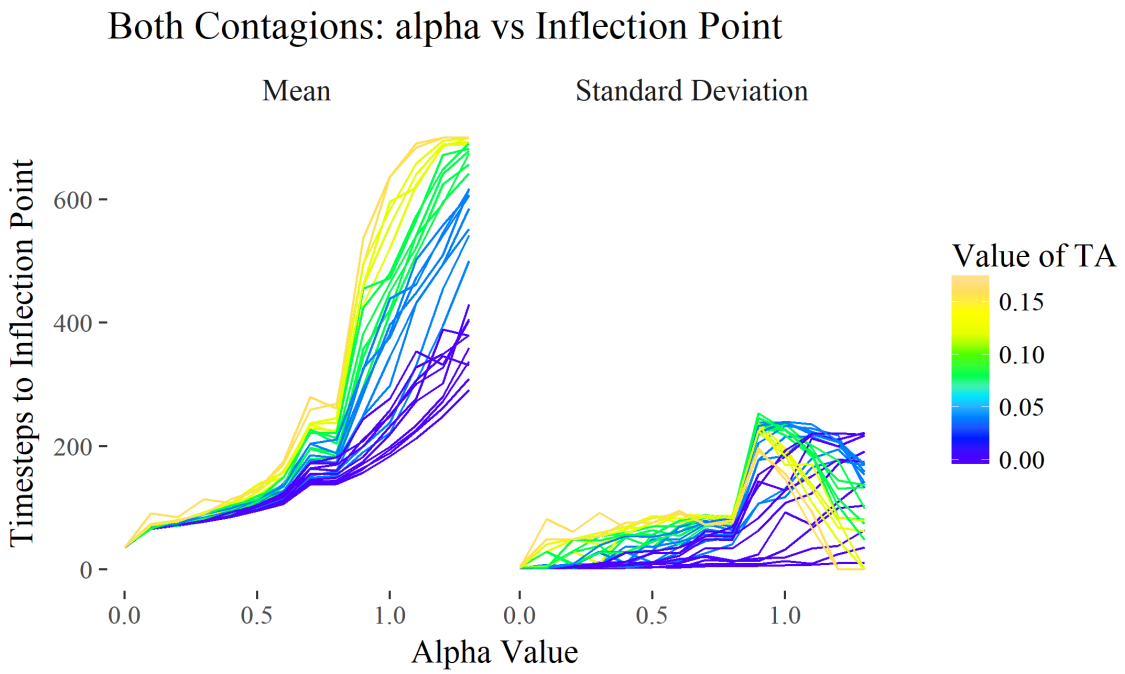

Figure 4.3: Rate of Diffusion increases with Alpha
The mean rate of diffusion (left) increases as α increases save a small plateau where $\alpha = 0.8$ and $\alpha = 0.9$. The standard deviation (right) remains stable until $\alpha = 0.9$.

it takes for diffusion to occur, the more time it allows nodes to gain dormancy and thus reduce the maximal depth of penetration.

We are now ready to address the central topic of the study: how do intrinsic parameters of A influence the diffusion of B? Figure 4.4 depicts the effects of increasing τ_A while holding constant α and τ_B, where $\alpha = 0.9$ and $\tau_B = 0$. When $\tau_A = 0$, Contagion A and Contagion B are equivalent and thus overlap each other. When $\tau_A = 0.02$ there is a drop in the ceiling of Contagion B from maximal diffusion to around 5,500. How can the adjustment of an intrinsic parameter of A affect B? We move on to When τ_A is further increased to 0.12. A certain proportion of Contagion B returns to its previous curve. This can be observed in the two diffusion graphs on the left, by matching the upper yellow curve when $\alpha = 0.12$ with the original yellow

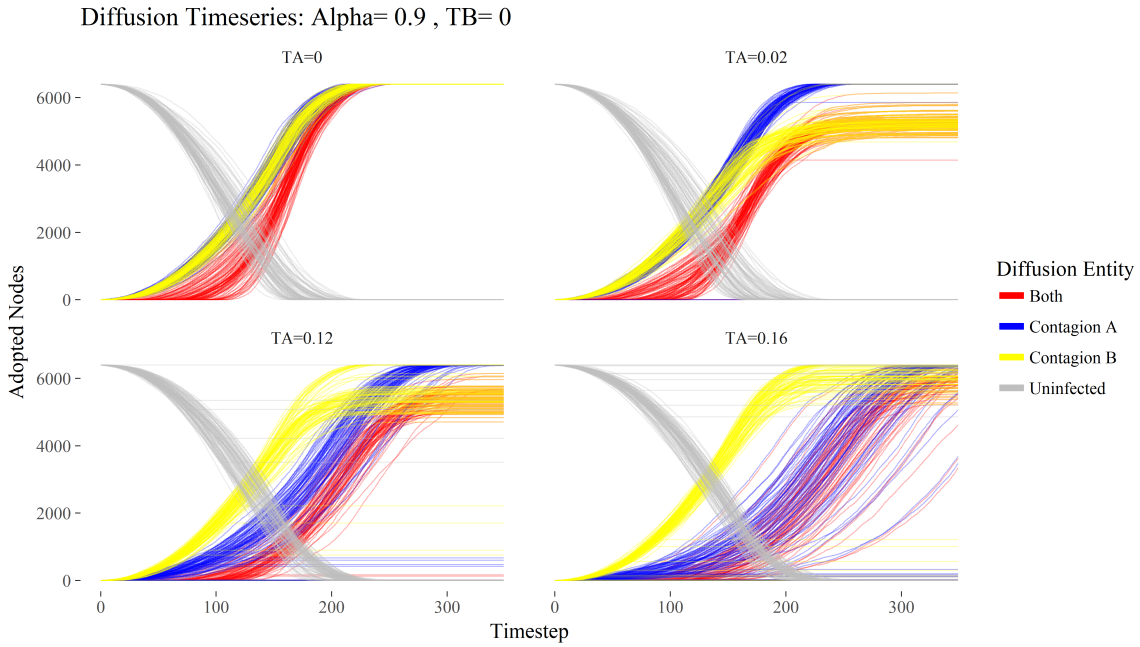

Figure 4.4: Diffusion Curves while Varying τ_A
The value of τ_A increases from 0 to 0.16. This first produces a bifurcation when $\tau_A = 0.02$, then as diffusion of A slows the curve for Contagion B returns to its original state.

curve when $\alpha = 0$. When $\tau_A = 0.16$ then most of the Contagion B diffusion curves return to their previous shape albeit with more variance in its ceiling. It cannot be simply concluded based on Figure 4.2 that the ceiling decreases uniformly as α increases. Rather, when coupled with τ it splits the ceilings of the other contagion into clusters, containing both the original curve and new curves that converge to a diminished ceiling. This is known as bifurcation. This effect can be seen clearly in Figure 4.8 of the next section.

Figure 4.3 is the key to understanding this phenomenon. While this depicts the diffusion curve of A and B, the effect of τ_A is equivalent on Contagion A itself. As τ_A increases, the rate also increases, marginally when α is small but much greater when $\alpha > 0.8$.

So far, we've established two facts. First, τ_A and τ_B lower the ceilings of τ_A and τ_B respectively by introducing "immunity" within the population. Second, τ_A influences the Contagion A's rate of diffusion. Now we turn our eye to the diffusion curves of Figure 4.4 again. When $\tau_A = 0.02$ the rate of diffusion curve of A does not decrease by much. This is evident as the blue curve does not shift to the right appreciably. However, nodes infected by A no longer participate in the diffusion process and thus the penetration depth of B is diminished. When τ_A is high, the rate of diffusion of Contagion A slows down sufficiently such that Contagion B diffuses more quickly and can thus fully diffuse.

The importance of primacy within the sequence of diffusion has thus become evident. If Contagion A diffuses more quickly, then the immunity towards participation it creates will diminish the diffusion of B as shown in the top right of Figure 4.4. Meanwhile, if Contagion A diffuses more slowly than B, and if $\tau_B = 0$, then both innovations will fully diffuse, as shown in the bottom right of Figure 4.4. This fact is perhaps the most interesting observation of the study, and it also explains the plateau and dip in Figure 4.3 that is accompanied by an increase in the standard deviation. When bifurcation in the diffusion curves takes effect, a large portion of the curves have diminished ceilings. Since the inflection point depends on the ceiling, the time it takes to reach that point *decreases*. Thus, the rate of diffusion increases because the ceiling decreases.

In fact, this instability can produce more than two clusters. As shown in the kernel density estimate of Figure 4.5, a tri-modal distribution is possible, where we vary τ_B relative to τ_A. When $\tau_A = \tau_B = 0.04$ the distribution remains bimodal, and the graph shows that Contagion A diffuses either completely or almost not at all. The reason why contagions do not spread far is because of percolation— the immunity

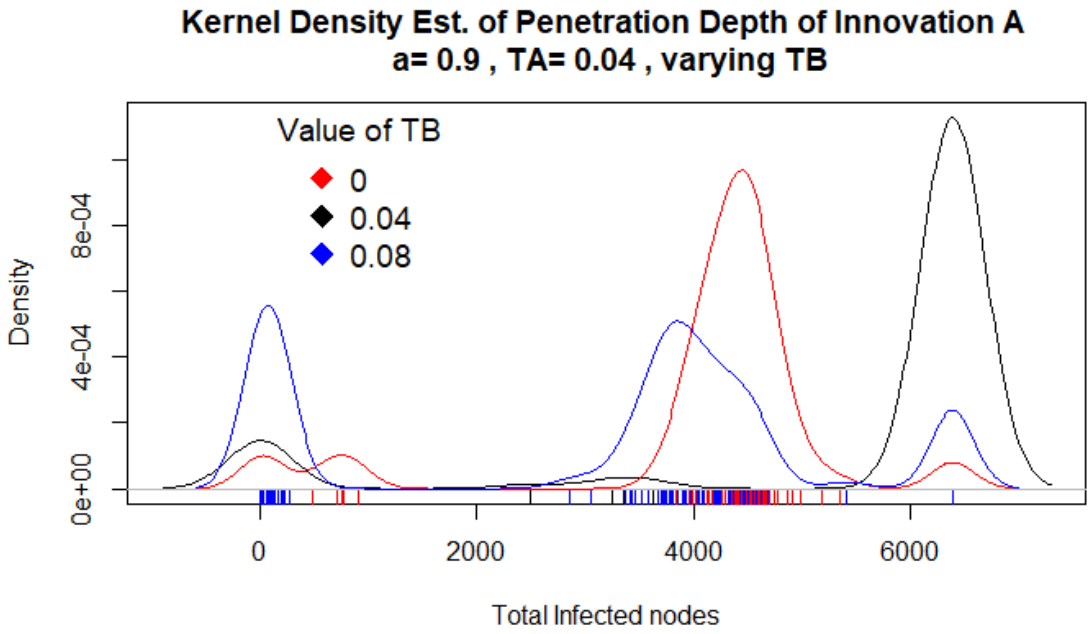

Figure 4.5: Kernel Density of Lattice Ceilings
A difference of 0.04 between τ_A and τ_B produces a tri-modal distribution of ceilings, while when they are equal the distribution is bi-modal.

decreases the participating active neighbors and thus restricts the innovation from spreading from its spatial origin. When $\tau_B = 0.08$ or when $\tau_B = 0.00$ a central cluster appears in addition to that of no diffusion and that of full diffusion. We can thus conclude tri-modality occurs when $\tau_A >> \tau_B$ or $\tau_A << \tau_B$, which is further shown in Figure 4.6. In the last row, the greatest regions of instability marked in red are regions where one τ is low and the other is high, which creates a large difference in τ. In the context of diffusion even a difference of 0.01 between the two values is quite significant.

It should be noted that the diffusion curve for both innovations will always be bound from below by the slower diffusing innovation. Referring back to Figure 4.4 we observe that the red never extends past the yellow curves or blue curves. The

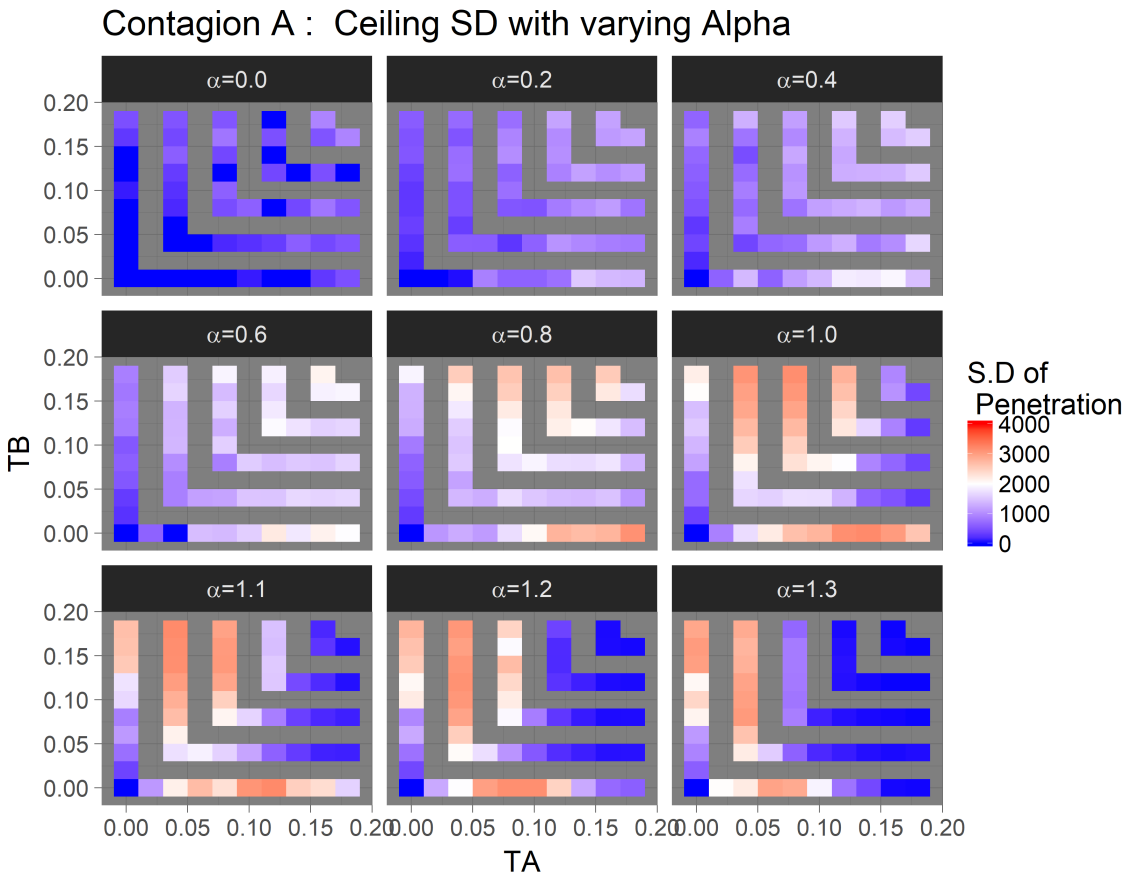

Figure 4.6: Ceiling Standard Deviation for Contagion A

red curve is thus minimum function that captures the lower cluster, given that all nodes are infected by at least one contagion. I show in Figure 4.7 the symmetry of the diffusion ceiling. As α increases and diffusion slows, the ceiling diminishes and is compressed towards $\tau_A = \tau_B = 0$, which by the logic of the previous discussions will always diffuse fully with sufficient time-steps. In other words, Contagion A affects the diffusion curve of both A and B the same way Contagion B does.

Lastly, it is useful to note that these observations on average agree with the mean-field equations derived in Chapter 3. Logically, the slower the rate of diffusion ϕ, the more nodes will be inactive at each stage of the diffusion process and thus the overall

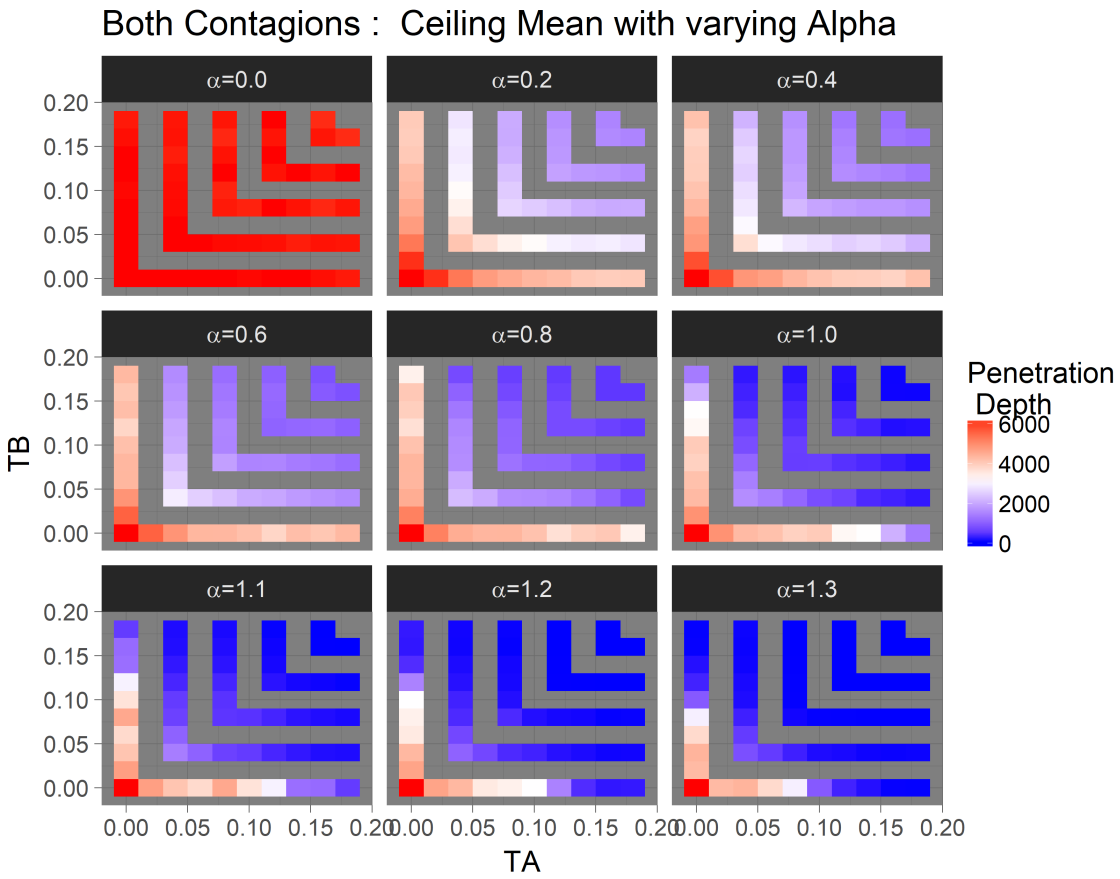

Figure 4.7: Ceiling Mean for Both A and B
The ceiling mean of state AB is symmetric.

ceiling will be lower. Furthermore, the mean-field equations can produce bi-stability as well. Figure 4.7 shows the lowering of the ceiling as either τ_A or τ_B is increased. Since τ_{AB} is defined as the mean of τ_A and τ_B it makes sense that the white line has a slope of -1 by symmetry. Additional heat-maps are provided in the Appendix.

4.2 Multiplex Diffusion

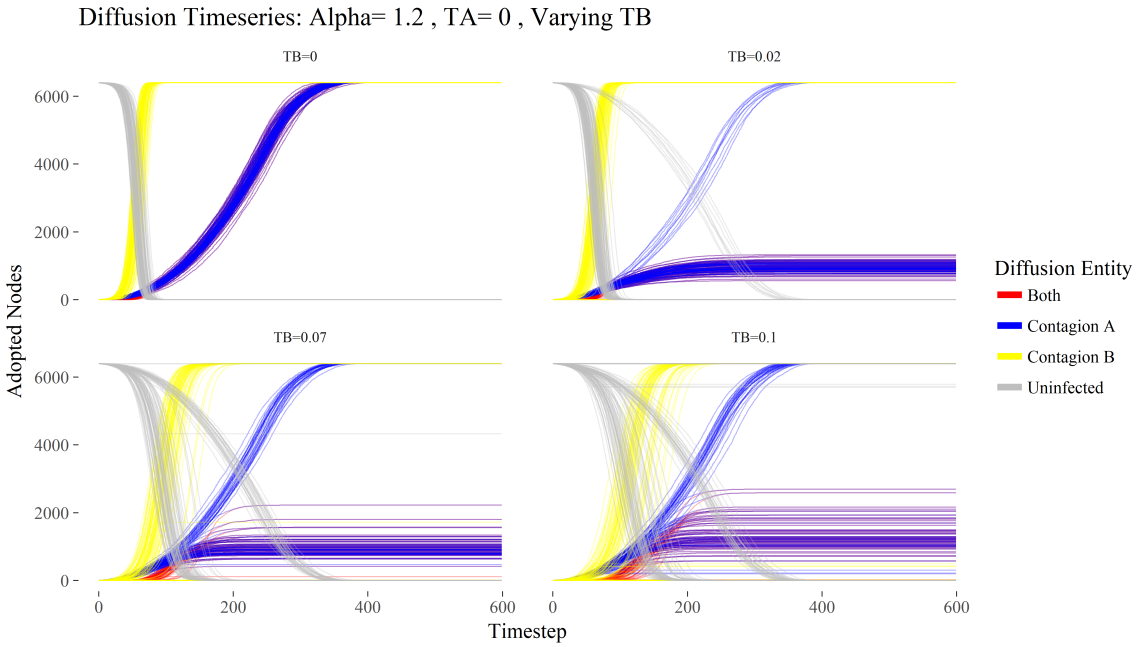

Figure 4.8: Multiplex Diffusion Curves while Varying τ_B
Introducing dormancy through τ_B produces a bifurcation.

Unlike the characterization of Contagions A and B in the lattice model, the two contagions are no longer equivalent because they diffuse on different layers of the multiplex network. Thus, analysis of just Contagion A is insufficient to draw conclusions about Contagion B and analysis of all three states (A, B, and AB) is required. Diving directly into the diffusion curves in Figure 4.8, we immediately observe that the diffusion of Contagion B (yellow) on the random-regular-graph is much faster than the diffusion of Contagion A (blue) on the lattice graph. This can be attributed to two advantages of long-range connections. First, as the diffusion process starts the uninfected nodes that Contagion B is in contact with is much greater than that of Contagion A. The uninfected nodes that Contagion A affects are always restricted to some physical front as seen in the left-most figure of 3.1, like the propagation of a

wave. Secondly, the long-range connections reduces the effect of percolation produced by τ_B. In contrast, restricting diffusion to von Neumann neighborhood encourages local percolation since many of the naive individuals share neighbors. This increasing the chance that a mutual neighbor no longer participates and thus decreasing the density-based adoption probability on the overall front.

We noted in the previous section that the first contagion to diffuse causes the second contagion to bifurcate. Since Contagion B diffuses faster on the random-regular-graph than Contagion A on the lattice, having $\tau_B > 0$ splits the diffusion curves of A. However, as τ_B increases from 0.02 to 0.07, the diffusion of B slows and more instances where Contagion A diffuses fully appear. This is shown by the greater density of the blue curves that diffuse fully. They converge to the original curve in the top left when $\tau_B = 0$, since T_B only affects the diffusion rate of B.

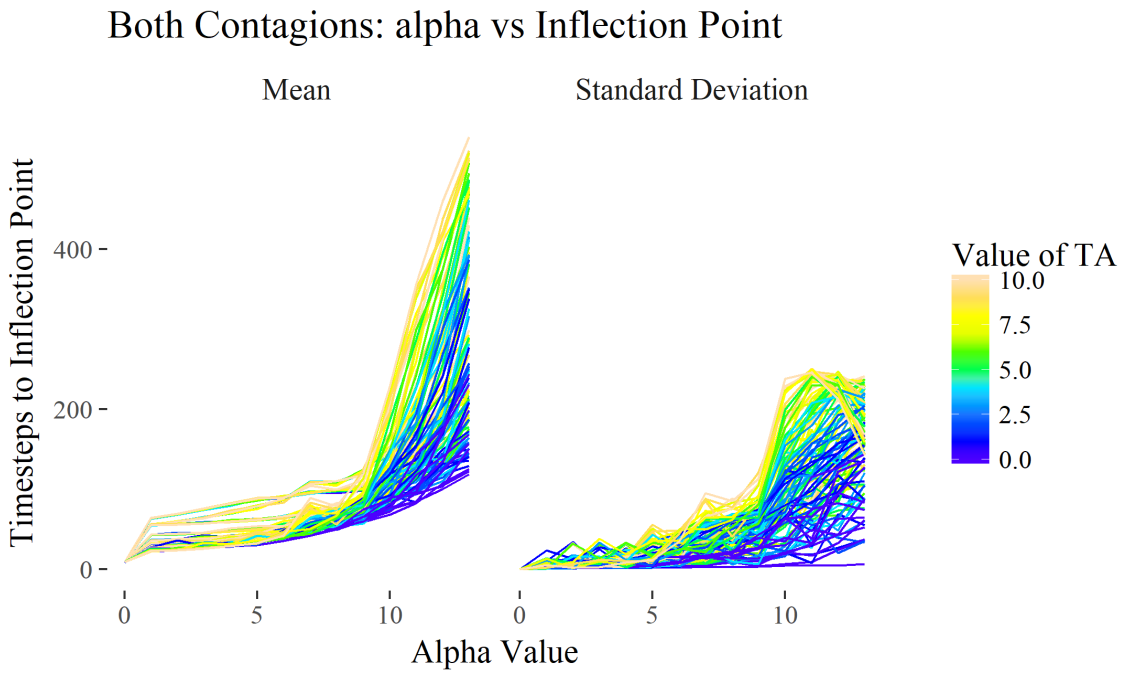

Figure 4.9: α slows diffusion for Multiplex

Figure 4.9 is analogous to Figure 4.3 and shows α as a shape parameter decreasing the rate of diffusion. It has more lines due to more parameters tested in the grid-search. It is tempting to say that by analyzing interdependent network diffusion where one contagion spreads faster than the other, we do not need to adjust the shape parameter K. K can be interpreted as the "attractiveness" parameter, which increases or decreases the rate of diffusion. However, since experiment 1 occurs on a single layer lattice it does not account for the difference in topology. Thus, we can only draw the conclusion that the way Contagion B impacts A the same way in both experiment 1 and 2, is if Contagion B spreads sufficiently faster than A such that their interaction is minimal.

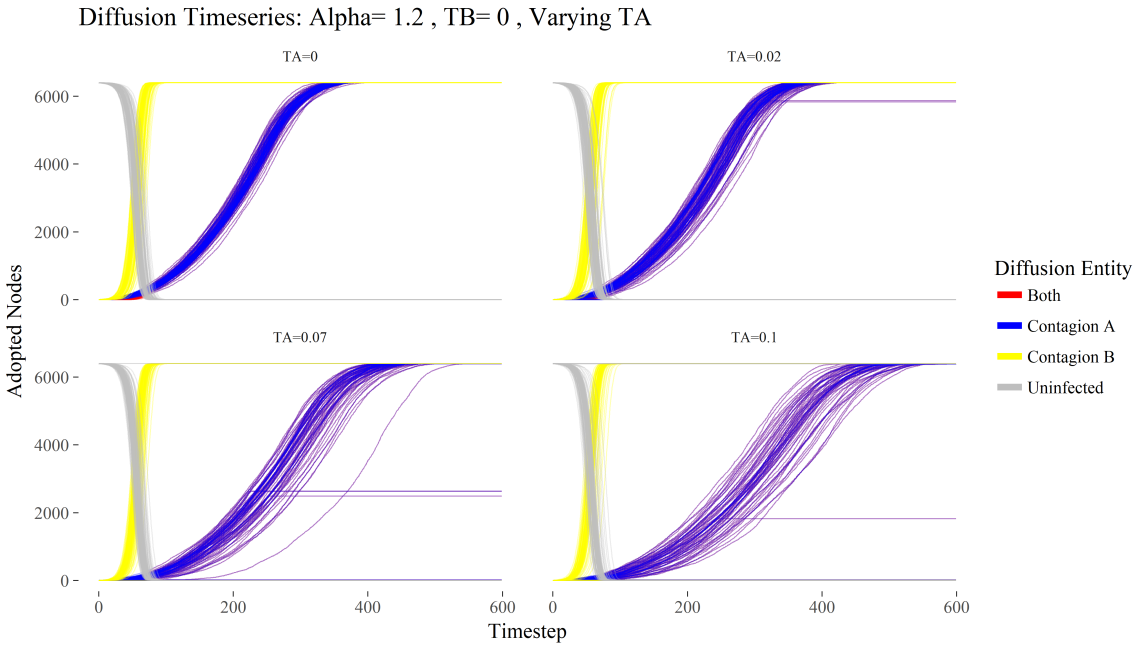

Figure 4.10: Multiplex Diffusion Curves while Varying τ_A
τ_A destabalizes the diffusion rate but most curves still diffuse completely despite percolation.

Another way to interpret the diffusion curves is that once B has fully diffused, then A is diffusing on a network where each node has a τ_B chance of switching off

at each time-step. The model then reduces to the case of single contagion diffusion on a graph where nodes gain spontaneous dormancy at a rate of τ_B. Furthermore, due to the random-regular-graph's much faster diffusion, if we set $\tau_B = 0$ then we eliminate the potential interference of dormancy and can thus analyze the effects of τ_A on Contagion A directly. This is shown in the top left of Figure 4.10.

As we intuited previously, Contagion A diffuses completely for the most part. The exceptions that don't are derivative of its own dormancy preventing sufficiently fast diffusion. Having established what we can expect from holding one τ equal to zero, we can begin to address the interaction of τ_A and τ_B with heat maps.

When $\alpha = 0$ the diffusion probability is uniformly 0.5 as shown in the top left of Figure 4.11. Diffusion is both constant and rapid which forces Contagion A to converge maximally. This is similar to the case of single layer diffusion. As α increases and diffusion slows, τ_B has a very pronounced effect on the ceiling. Consider the case when $\alpha = 0.2$ and τ_B jumps from 0.02 to 0.03. The mean ceiling diminishes rapidly shown by the color change of red to white. As α increases the decrease in ceiling mean is even more pronounced, which produces the very noticeable color jump between $\tau_B = 0$ and $\tau_B = 0.01$. This rapid drop in ceiling is a testament to how much faster τ_B diffuses, where even low values of τ_B have sufficient time to inject dormancy into the populace.

Consider the last row of the grid where $\alpha = 1.1,\ 1.2$ and 1.3. When we hold each τ_B constant we observe a gradient effect left to right from increasing τ_A. This is most pronounced when $\tau_B = 0$. We conclude that if $\alpha > 1.0$, then τ_A has a large effect on the ceiling of Contagion A.

The previous two observations on τ_B and τ_A respectively allows us to conclude that increasing α essentially compresses the graph from the right and from the top.

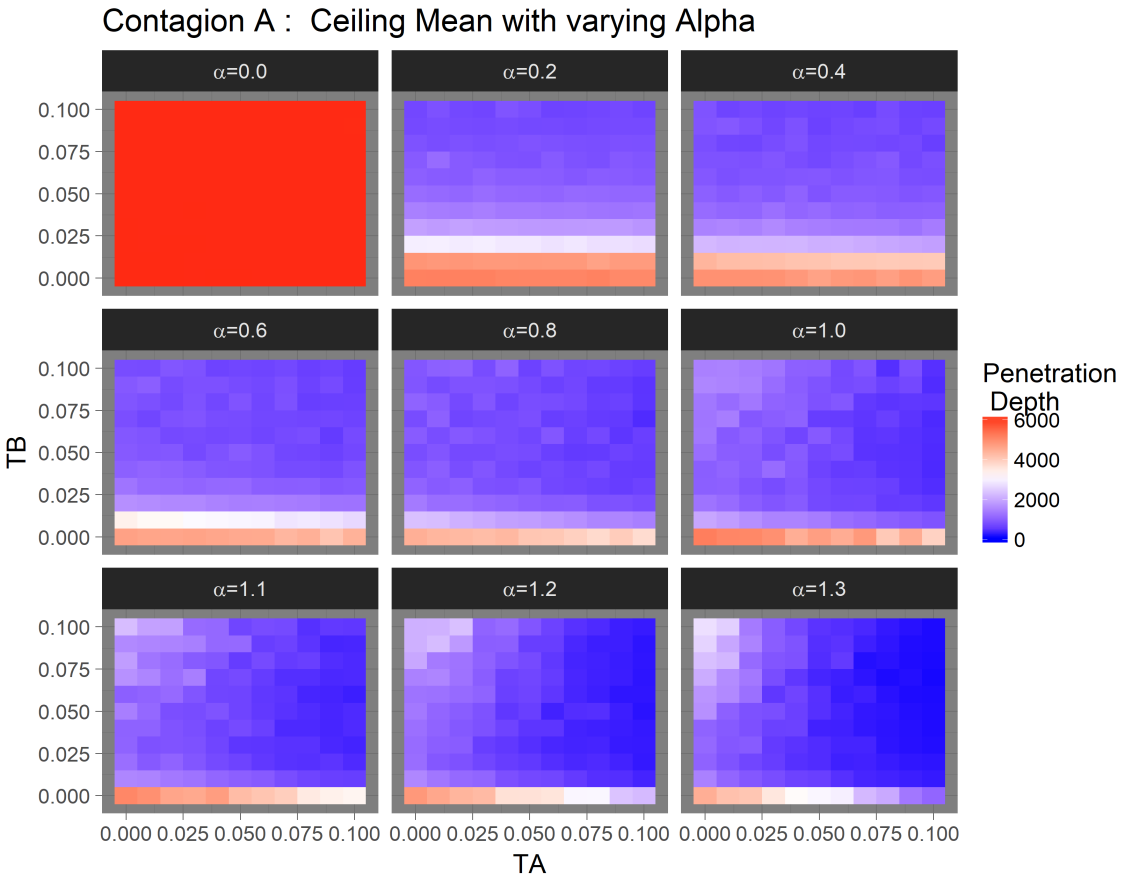

Figure 4.11: Ceiling Mean of Contagion A for Multiplex Experiment
The ceiling of A demonstrates high sensitivity to τ_B when $\alpha < 0.8$. It shows sensitivity to τ_A when $\alpha > 1.0$

The two red horizontal rows in the $\alpha = 0.2$ grid is eventually compressed into one row from above. The horizontal gradient of $\tau_B = 0$ and $\alpha = 1.1,\ 1.2$ and 1.3 (bottom row of the grid) is compressed towards the left. α increases the timescale of the diffusion by increasing the slope of the Hill-curve, which gives τ_A and τ_B more time to produce dormancy although they demonstrate different sensitivities towards α.

When τ_B is high the ceiling of A actually increases. This phenomenon is due to τ_B slowing the diffusion of Contagion B, which produces more bifurcated "upper" curves of Contagion A, and we can see this in Figure 4.8 by comparing $\tau_B = 0.02$

and $\tau_B = 0.1$. I show more intuition for this phenomenon when I discussion of Figure 4.15. Since the diffusion curve of AB is bounded from below by the slower diffusion contagion, the ceiling heat-map of Contagion A and AB are almost identical. The heat-map for AB can be found in Figure A.2 of the Appendix.

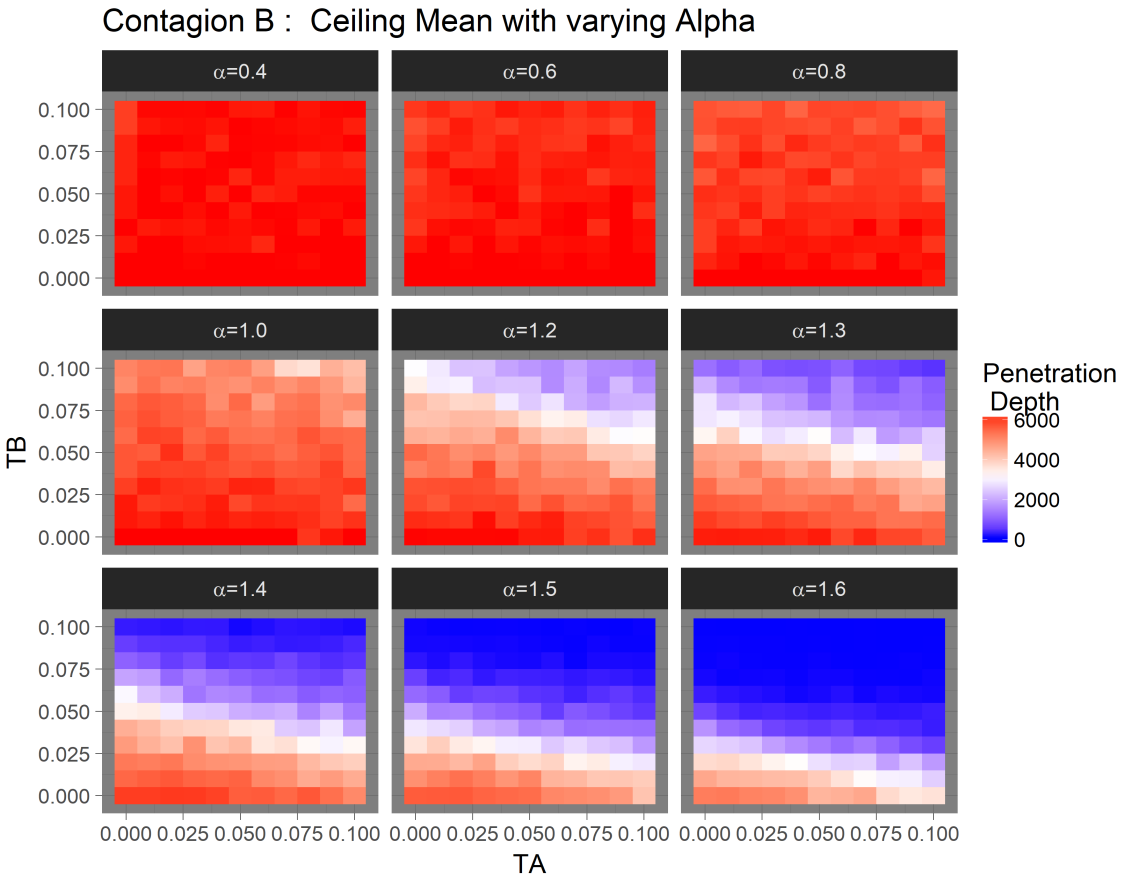

Figure 4.12: Multiplex Ceiling Mean of Contagion B
The white line indicates a linear relationship to Contagion B's ceiling sensitivity

Contagion B produces a very different looking heat map. Given its fast diffusion it penetrates fully or close to fully for $\alpha < 0.8$. Then, a diagonal white line moves from the top right downwards and compresses towards the bottom left. The slope of this white line and its spread can be interpreted as Contagion B's sensitivity to τ_A. In other words, it quantifies how much the dormancy constant of Contagion A

affects its own diffusion. In a similar vein, the prior heat maps are also sensitivity analyses and also show the dominance of τ_B. The effects of τ_A only come in play with sufficiently high α to slow the diffusion rate.

One observation is that in Figure 4.12 the block where $\tau_A = \tau_B = 0$ no longer denotes maximal diffusion. This is because we used a subset of data where Innovation B does not reach full diffusion ($\alpha > 1.4$) to show this effect more clearly, but it converges to the same result.

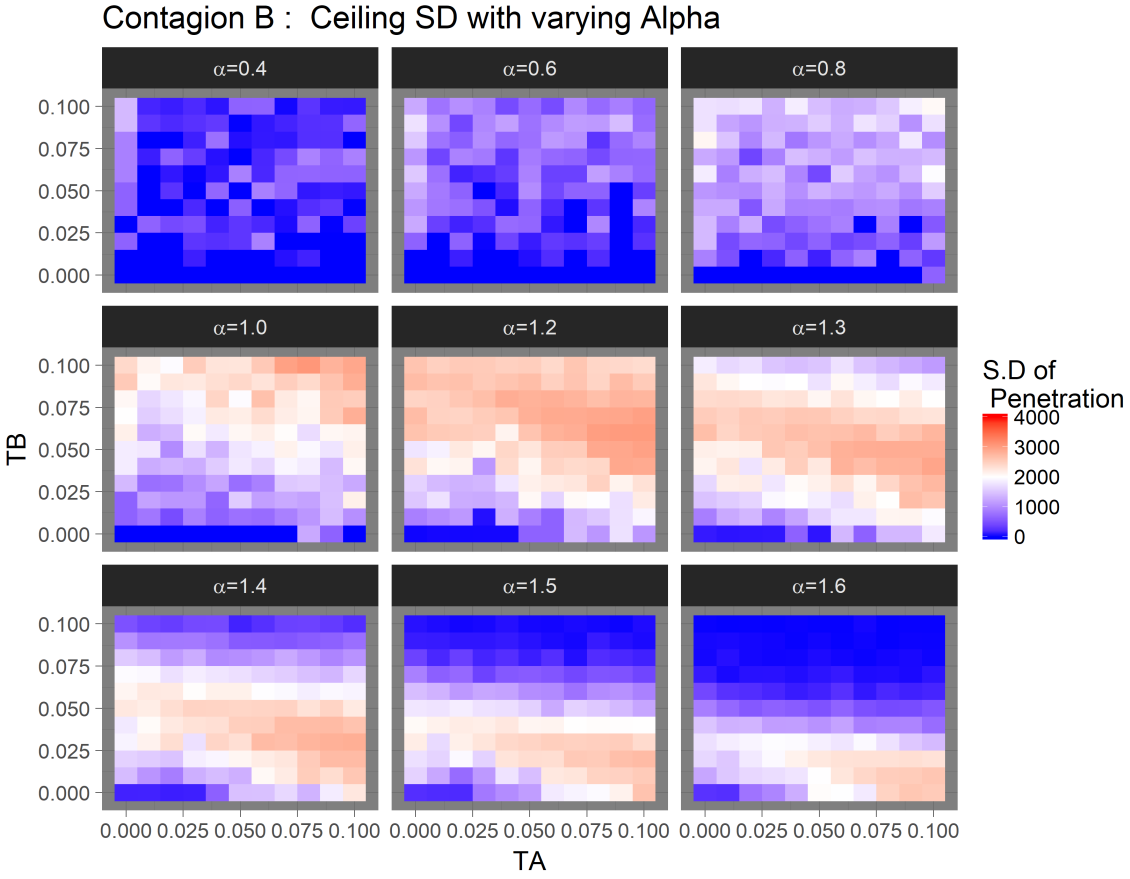

Figure 4.13: Multiplex Ceiling Standard Deviation of Contagion B
The standard deviation for Contagion B is greatest along the line in Figure 4.13

Once again, averages do not paint the full picture. Having established that bifurcation occurs we are interested in pinpointing the specific conditions that induce such

instabilities. Instabilities can be inferred from high levels of standard deviation and we consider instability of Contagion B shown in Figure 4.13. The region of highest instability shown in red overlaps with the white line shown . This is particularly evident in the last row where $\alpha = 1.4$ to 1.6. The region of the line becomes compressed and is sandwiched between two blue areas. The blue zone in the bottom left denotes the cases where Contagion B fully diffuses, the blue zone above denotes the case where Contagion B does not diffusing at all due to percolation produced by the high value of τ_B. Increasing α produces the compression effect towards $\tau_A = \tau_B = 0$ from above as timescale increases.

One implication of the Contagion B heat-map for standard deviation is that, unlike the lattice diffusion experiment, instabilities for Contagion B not only occur when $\tau_A >> \tau_B$ or $\tau_B >> \tau_A$, but on any point of the white line. For instance, with each parameter set denoted with the tuple $(\alpha,\ \tau_A,\ \tau_B)$, the outcome of $(1.6,\ 0.00,\ 0.04)$ is equal to $(1.6,\ 0.10,\ 0.02)$, although there is greater instability in the latter case when $\tau_A = 0.10$.

For the Contagion A however, we observe that in comparison with Contagion B the strongest nonlinearities occur once more when $\tau_A >> \tau_B$ or $\tau_B >> \tau_A$, shown in Figure 4.14. However, τ_B influences the diffusion variance of A for many low values of τ_A, shown by the top-left white region when $\alpha > 1.0$. In comparison, the effect of τ_A is most pronounced when $\tau_B = 0$. This does not mean τ_A does not influence the variance for other values of τ_B, but rather it's not a sensitive variable. In other words, the dormancy variable of Contagion B influences the ceiling of Contagion A greatly because of its diffusion primacy. Once more, we observe the "compression" effect towards $\tau_A = \tau_B = 0$ from increasing α. Note that that square is uniformly blue because both Contagion A fully diffuses.

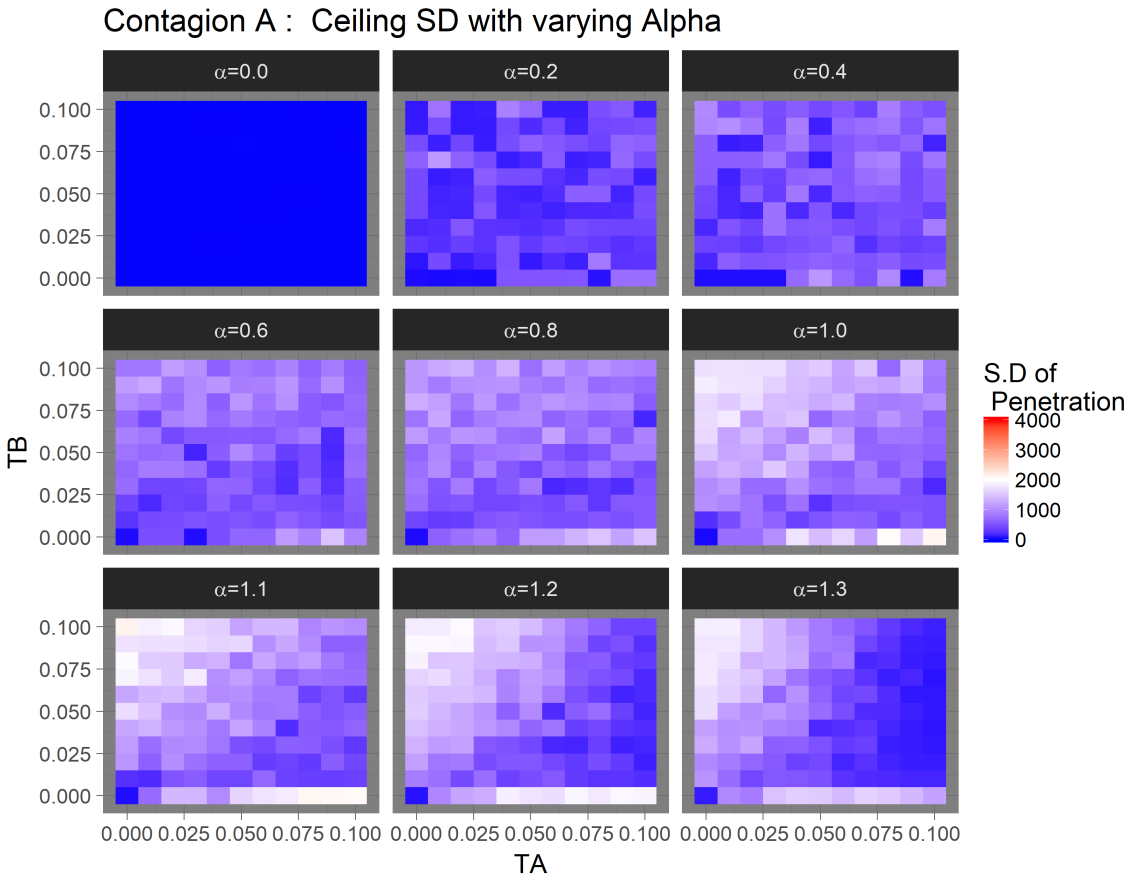

Figure 4.14: Multiplex Ceiling Standard Deviation of Contagion A

Lastly, we consider when both values of τ are non-negative and analyze their interaction. Figure 4.15 demonstrates the interaction of τ_A and τ_B where we set low values equal to 0.01 and high values at 0.1. When both τ_A and τ_B are low, both converge to one cluster of ceilings. When τ_A is low and τ_B is high, the splitting effect is most pronounced. In fact, the number of Contagion A curves that split upward is equal to the number of Contagion B curves that diffuse slower than it. However, it should be noted that for the most part even when Contagion B diffuses slower than Contagion A, it does not partial diffuse when α is sufficiently low, since it is not affected by local percolation. To see this effect more clearly, refer to Figure A.3.

This qualification is required as the heat map in Figure 4.12 shows that percolation can still occur to Contagion B when τ_B and α are sufficiently high.

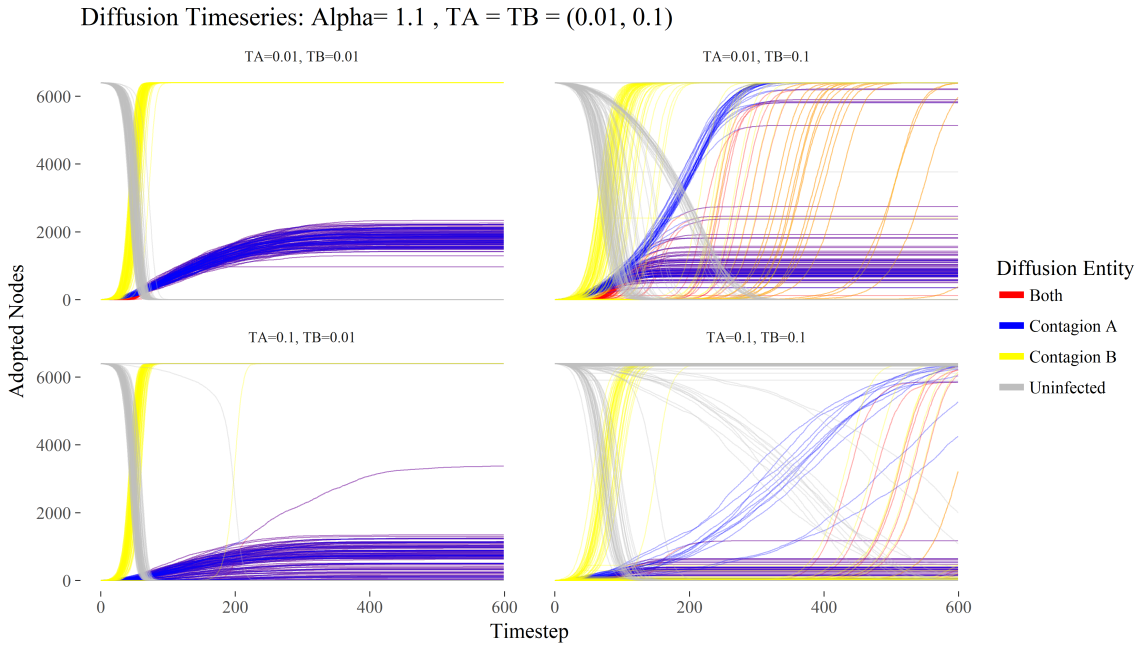

Figure 4.15: Interaction of τ_A and τ_B

Chapter 5

Conclusion

5.1 Summary of Results

The objective of this study is to investigate the properties of a newly proposed diffusion model by simulating two social contagions interacting on a periodic lattice in Experiment 1 and a multiplex network in Experiment 2. These contagions are parametrized based on shape parameters α and K, and their intrinsic dormancy τ_A, τ_B and τ_{AB} for states A, B and both A and B respectively. Their relative attractiveness K is set to be equal, and τ_{AB} is assumed to be the arithmetic mean of τ_A and τ_B.

We have determined how the parameters broadly influence the level of diffusion. Increasing α increases the time of diffusion. Without loss of generality, the stochastic dormancy constants τ_A lowers the penetration depth of Contagion A, and perhaps surprisingly also Contagion B. We conclude that primacy is important in this model of co-diffusion. Furthermore, if Contagion A diffuses more quickly, it will most probably attain maximal penetration. If it diffuses more slowly than Contagion B, then it is

subject to partial diffusion. This is due to the dormancy introduced by the initial passage of Contagion B through the populace.

I hypothesized that the parameter set ($\alpha,\ \tau_A,\ \tau_B$) is highly nonlinear; I can now state how the nonlinearity manifests in different topological settings. Starting with the single layer lattice, the decrease in the penetration depth of A caused by the first passage of B is non-uniform. Rather, it bifurcates into two or three clusters based on the ratio τ_A to τ_B for a set range of α. Generally, when the difference between τ_A and τ_B is large within the region of $0.8 < \alpha < 1.3$, a bifurcation is expected. There is an even split between clusters when the difference is large because, without loss of generality, an increase in τ_A corresponds to a large decrease in the rate of diffusion for A. The effect is marginal when $\alpha < 0.8$, but grows greatly when $\alpha > 0.8$ (as shown in Figure 3.3).

In the multiplex network, given that K are equal, Contagion B diffuses much faster than Contagion A . It's faster diffusion is due to two reasons. First, the random-regular-graph's larger diffusion front compared to the lattice's, which is constrained physically. Second, it's diffusion is not constrained by local percolation. As we know, when B diffuses first it diffuses fully to 6400 nodes. Interestingly, in the cases where B diffuses after A, it will still diffuse fully to whatever maximum that A sets. Contagion A on the lattice sets the minimal ceiling.

5.2 Applications

As I mentioned in the beginning, one critique of agent-based modeling is that its reductivism diminishes its utility and applicability. The interpretation in biology is clear: two diseases help each other spread by synergistically weakening the immune

system of individuals, but once a certain number of hosts recover, the second disease has a harder time penetrating the populace due to diminished density. However, there are applications outside of biology. Here, I offer some potential ways to interpret these results, in particular the notions of synergy and dormancy, in the areas of social science mentioned in the literature review in Chapter 2.

5.2.1 Innovation Diffusion of Blockchain

Blockchain technology has recently been considered as a potential general purpose technology [8] [30] [13]. The application of blockchain to cryptocurrencies, or Bitcoin, spurned a large wave of interest and investment in 2017 [7] [6].

Given the speculation surrounding cryptocurrency, this investment behavior can certainly be categorized as a social contagion [53]. While cryptocurrency theoretically serves as means substance for transactions, current investors treat it more as a commodity or asset, rather than as liquid money. In that regard, the adoption of cryptocurrency is not dissimilar to a firm's adoption of a general-purpose technology to increase output. In essence, there is an investment in the GPT, then an expected benefit or return from the adoption.

If you are an investor with a finite portfolio, there are two questions that naturally arise. First, do you adopt the technology and invest in Bitcoin? Second, which cryptocurrency do you choose to invest in?

The first question corresponds to Equation 3.5, where all cryptocurrencies synergistically contribute to the diffusion of the adoption behavior. The second question refers to the coin-flip in Equation 3.6, which frames individual cryptocurrencies as competitors. However, this does not preclude the possibility of adopting the one not chosen at a future time. In this regard, the diffusion mechanism of this thesis captures

both cooperative and quasi-competitive aspects of the technology that was mentioned by Chandrasekaran [10] in Chapter 2.

5.2.2 Cultural Dissemination across Distance

Beyond the diffusion mechanism, this topology offers a natural extension to Axelrod's cultural diffusion model. Cultural dissemination is no longer confined to physical geography. As stated in Section 2.1.2, contemporary research has shown that emergent phenomenon differ on different graph structures. Models of modern cultural dissemination should contain multiple conduits for information, and have both long-range and local connections.

Additionally, my model offers another way to model the traits in Axelrod's model by treating them as diffusing contagions. Similarity between agents is defined by how many features they share, but there is no spectrum in which the features fall on, and thus it does not consider features that are more or less similar to one another. In contrast, the current model allows for the possibility of both A and B allow the model to capture a mixtures of discrete states. The dormancy variable would represent a resistance to changing traits. This formulation, while relying on a different set of assumptions, adds information to the model while keeping it tractable.

5.3 Future work

There are multiple pathways for future inquiry that build on the weaknesses in this study, specifically with shape parametrization, seeding, the diffusion mechanism, and graph topologies. In this study we assume the shape characterization of contagion adoption to be equal; that is, in our parametrization $K_A = K_B$. Changing this pa-

rameter would allow for a more in-depth study of the effects of primacy by controlling precisely how much faster one of the contagion diffuses relative to the other. Controlling for K_B would be meaningful for interdependent networks, such as controlling for the much faster diffusion on the random-regular-graph. For τ_A to restrain the diffusion of τ_B, B must diffuses slowly. Due to the difference in topology, the current parameter pairs are insufficient to consider the case where Contagion B diffuses slower than A.

Seeding may affect the diffusion, as there may be a relationship between the final diffusion curves and the distance between the seeds. Similarly, the timing of entry is an interesting question. Given that Contagion A diffuses first with a high value of τ_A, late entry by Contagion B would most likely affect its penetration depth. Quantifying this result would be useful for benchmarking the benefits or risks of late adaptation of general purpose technologies.

Different topologies would certainly yield different results. However, we have shown a difference in the diffusion of spatial and long-range graphs, for a model to accurately describe how social media and physical newspapers help each other spread news, more precise networks would have to be implemented. In this case, power-law graphs and lattice graph may be suitable. Methods for extracting the ceiling such as unsupervised learning to produce clusters would help understand the modality of convergent behavior.

Another avenue for research is modeling exclusive adoption as we have outlined in Section 3.4.3. Such a probability kernel for diffusion would be useful for modeling products that are purely competitive. For instance, two companies launch new phones, each embedded with a new and attractive feature. However, consumers typically only need one phone. As a result, while the feature they share help the new

phones diffuse synergistically in aggregate they still compete with each other. There are also many limitations to threshold models. Instead, a network coordination model could be be used to produce a more complicated, but still inherently rational diffusion mechanism.

Appendix A

A.1 Lattice

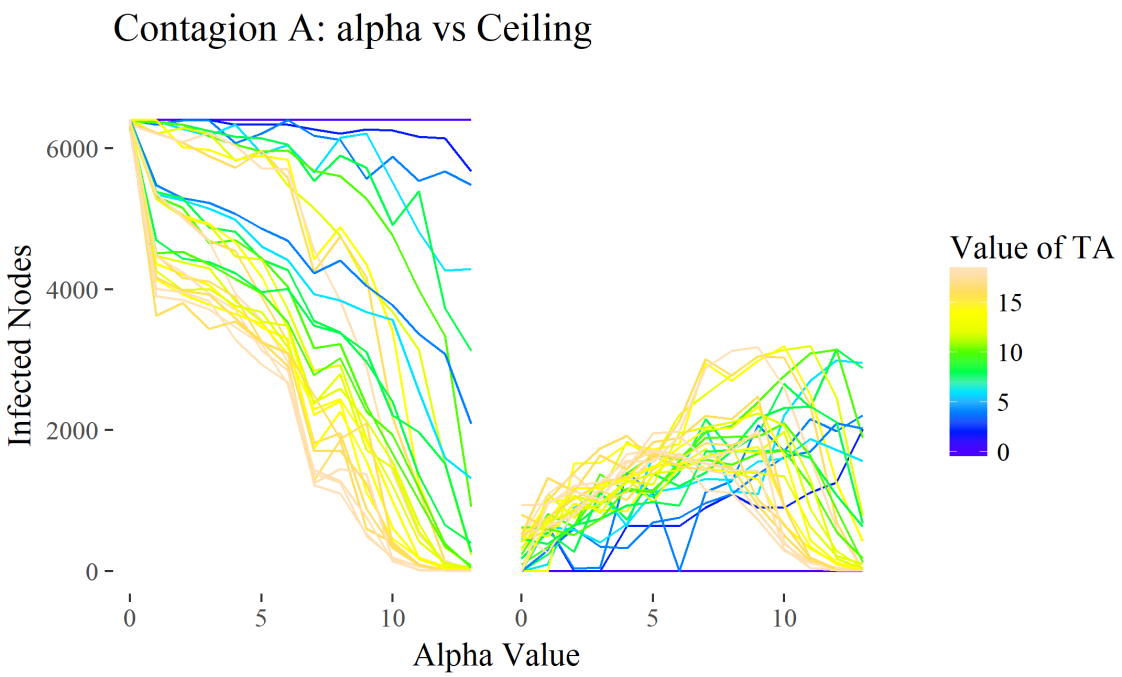

Figure A.1: Ceiling vs α for Contagion A
The ceiling of A decreases with α

A.2 Multiplex

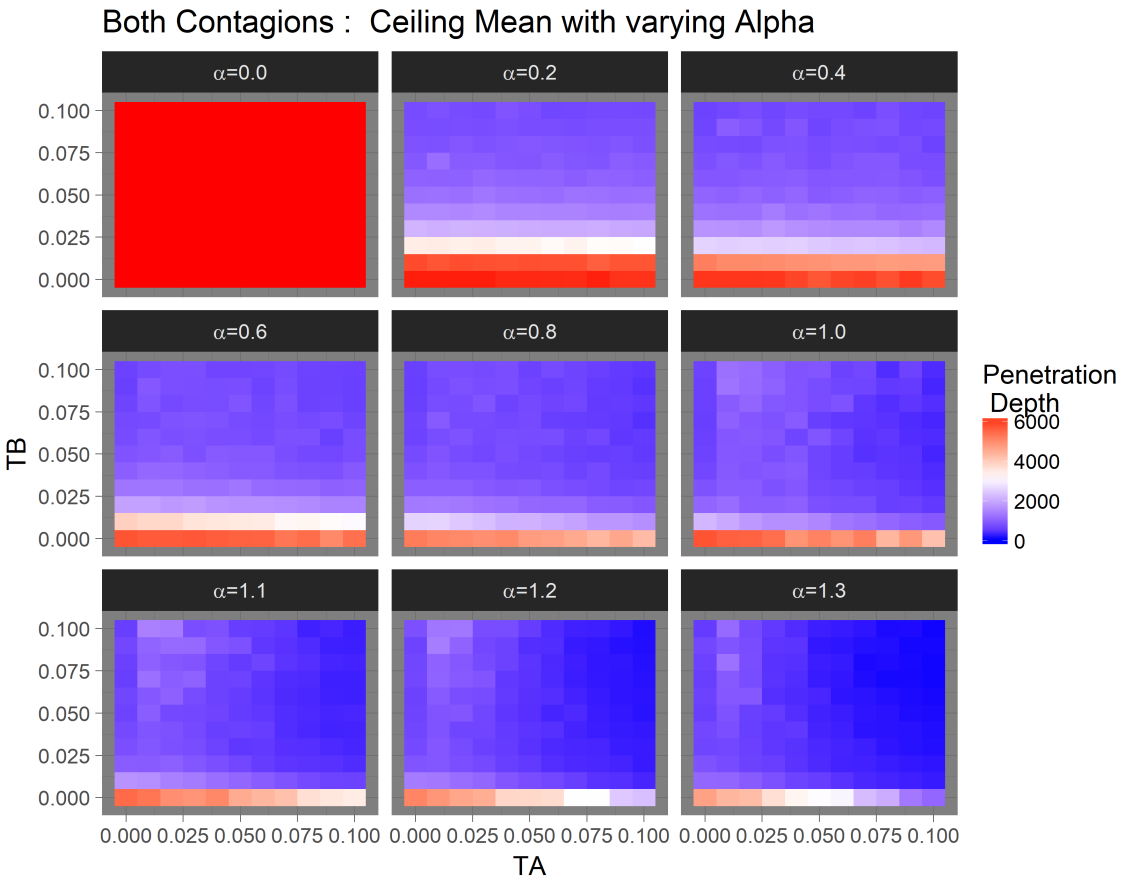

Figure A.2: Heat-map of Ceiling Mean of AB for Multiplex Experiment
The heat-map corresponds to the heat-map of Contagion A in Figure 4.11

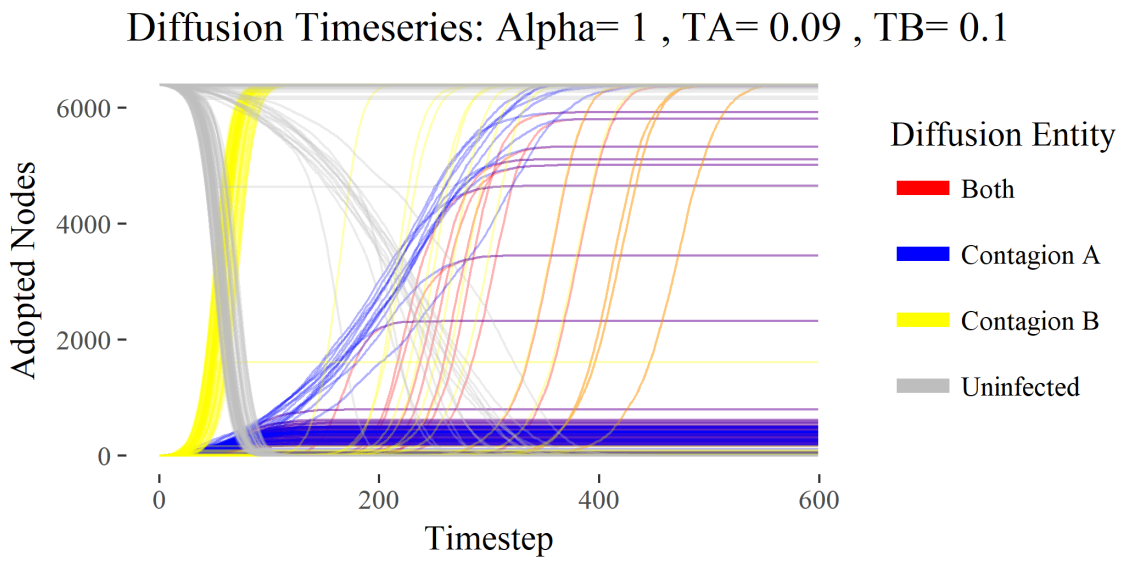

Figure A.3: Unstable diffusion without bifurcation from B
When Contagion B diffuses later than A it converges fully to the ceiling of A

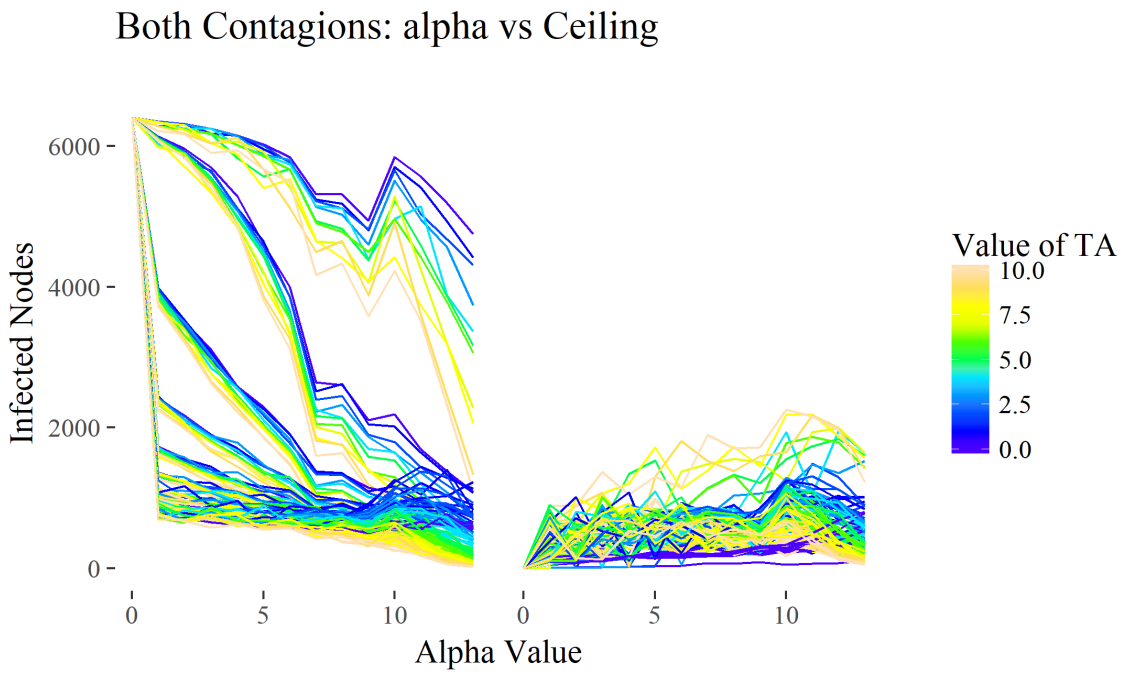

Figure A.4: Ceiling Mean vs α for AB

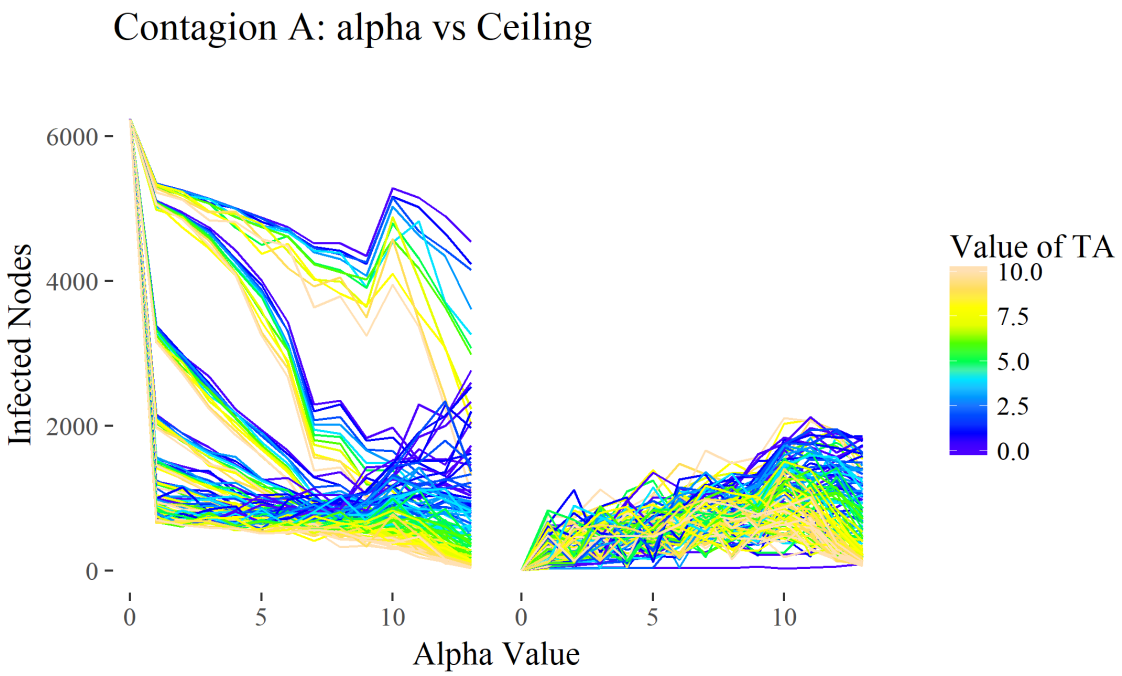

Figure A.5: Ceiling Mean vs α for A

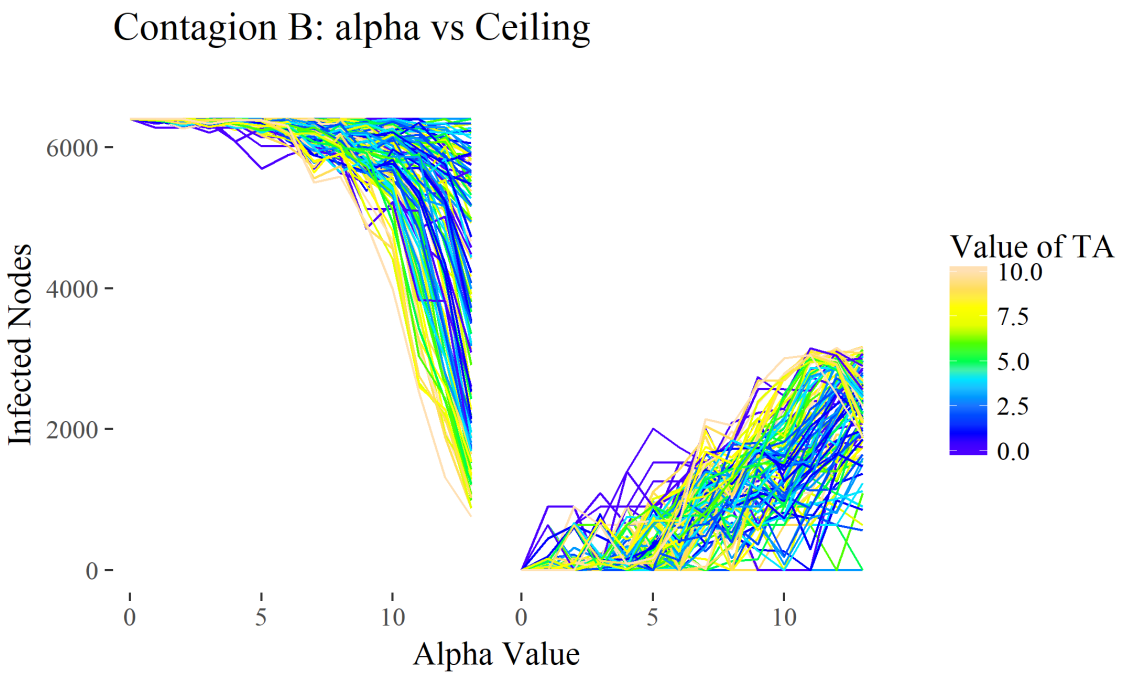

Figure A.6: Ceiling Mean vs α for B

References

[1] Alberto Aleta and Yamir Moreno. Multilayer networks in a nutshell. *arXiv preprint arXiv:1804.03488*, 2018.

[2] David Andolfatto and Glenn M MacDonald. Technology diffusion and aggregate dynamics. *Review of Economic Dynamics*, 1(2):338–370, 1998.

[3] Robert Axelrod. The dissemination of culture: A model with local convergence and global polarization. *Journal of conflict resolution*, 41(2):203–226, 1997.

[4] Frank M Bass. A new product growth for model consumer durables. *Management science*, 15(5):215–227, 1969.

[5] Ronald S Burt. Social contagion and innovation: Cohesion versus structural equivalence. *American journal of Sociology*, 92(6):1287–1335, 1987.

[6] Buy Bitcoin Worldwide. The bitcoin volatility index.

[7] Jon Carrick. Bitcoin as a complement to emerging market currencies. *Emerging Markets Finance and Trade*, 52(10):2321–2334, 2016.

[8] Christian Catalini and Joshua S Gans. Some simple economics of the blockchain. Technical report, National Bureau of Economic Research, 2016.

[9] Damon Centola, Juan Carlos Gonzalez-Avella, Victor M Eguiluz, and Maxi San Miguel. Homophily, cultural drift, and the co-evolution of cultural groups. *Journal of Conflict Resolution*, 51(6):905–929, 2007.

[10] Deepa Chandrasekaran and Gerard J Tellis. A critical review of marketing research on diffusion of new products. In *Review of marketing research*, pages 39–80. Emerald Group Publishing Limited, 2007.

[11] Li Chen, Fakhteh Ghanbarnejad, and Dirk Brockmann. Fundamental properties of cooperative contagion processes. *New Journal of Physics*, 19(10):103041, 2017.

[12] Robin Cowan and Nicolas Jonard. Network structure and the diffusion of knowledge. *Journal of economic Dynamics and Control*, 28(8):1557–1575, 2004.

[13] Sinclair Davidson, Primavera De Filippi, and Jason Potts. Economics of blockchain. 2016.

[14] Sebastiano A Delre, Wander Jager, Tammo HA Bijmolt, and Marco A Janssen. Will it spread or not? the effects of social influences and network topology on innovation diffusion. *Journal of Product Innovation Management*, 27(2):267–282, 2010.

[15] Peter Sheridan Dodds and Duncan J Watts. A generalized model of social and biological contagion. *Journal of theoretical biology*, 232(4):587–604, 2005.

[16] David Easley and Jon Kleinberg. *Networks, crowds, and markets: Reasoning about a highly connected world*. Cambridge University Press, 2010.

[17] Fredrik Erlandsson, Piotr Bródka, and Anton Borg. Seed selection for information cascade in multilayer networks. *arXiv preprint arXiv:1710.04391*, 2017.

[18] Joseph Farrell and Garth Saloner. Standardization, compatibility, and innovation. *The RAND Journal of Economics*, pages 70–83, 1985.

[19] Julie Foucquier and Mickael Guedj. Analysis of drug combinations: current methodological landscape. *Pharmacology research & perspectives*, 3(3), 2015.

[20] Juan Carlos González-Avella, Mario G Cosenza, Konstantin Klemm, Víctor M Eguíluz, and M San Miguel. Information feedback and mass media effects in cultural dynamics. *arXiv preprint arXiv:0705.1091*, 2007.

[21] Trisha Greenhalgh, Glenn Robert, Fraser Macfarlane, Paul Bate, Olympia Kyriakidou, and Richard Peacock. Storylines of research in diffusion of innovation: a meta-narrative approach to systematic review. *Social science & medicine*, 61(2):417–430, 2005.

[22] Antonio Ladrón de Guevara, Anita Elberse, and WP Putis. Diffusion of complementary products with network effects: A model with applications. In *36th MAC (European Marketing Academy) Conf. Proc*, 2007.

[23] Douglas Guilbeault, Joshua Becker, and Damon Centola. Complex contagions: A decade in review. *arXiv preprint arXiv:1710.07606*, 2017.

[24] Sachin Gupta, Dipak C Jain, and Mohanbir S Sawhney. Modeling the evolution of markets with indirect network externalities: An application to digital television. *Marketing Science*, 18(3):396–416, 1999.

[25] Alison L Hill, David G Rand, Martin A Nowak, and Nicholas A Christakis. Emotions as infectious diseases in a large social network: the sisa model. *Proceedings of the Royal Society of London B: Biological Sciences*, 277(1701):3827–3835, 2010.

[26] Alison L Hill, David G Rand, Martin A Nowak, and Nicholas A Christakis. Infectious disease modeling of social contagion in networks. *PLOS computational biology*, 6(11):e1000968, 2010.

[27] Dorit S Hochbaum, Erick Moreno-Centeno, Phillip Yelland, and Rodolfo A Catena. Rating customers according to their promptness to adopt new products. *Operations research*, 59(5):1171–1183, 2011.

[28] Raghuram Iyengar, Christophe Van den Bulte, and Thomas W Valente. Opinion leadership and social contagion in new product diffusion. *Marketing Science*, 30(2):195–212, 2011.

[29] Boyan Jovanovic and Peter L Rousseau. General purpose technologies. *Handbook of economic growth*, 1:1181–1224, 2005.

[30] Ethan Kane. Is blockchain a general purpose technology? 2017.

[31] David Kempe, Jon Kleinberg, and Éva Tardos. Maximizing the spread of influence through a social network. In *Proceedings of the ninth ACM SIGKDD international conference on Knowledge discovery and data mining*, pages 137–146. ACM, 2003.

[32] Maksim Kitsak, Lazaros K Gallos, Shlomo Havlin, Fredrik Liljeros, Lev Muchnik, H Eugene Stanley, and Hernán A Makse. Identification of influential spreaders in complex networks. *arXiv preprint arXiv:1001.5285*, 2010.

[33] Konstantin Klemm, Víctor M Eguíluz, Raúl Toral, and Maxi San Miguel. Global culture: A noise-induced transition in finite systems. *Physical Review E*, 67(4):045101, 2003.

[34] Konstantin Klemm, Víctor M Eguíluz, Raúl Toral, and Maxi San Miguel. Nonequilibrium transitions in complex networks: A model of social interaction. *Physical Review E*, 67(2):026120, 2003.

[35] Konstantin Klemm, Vıctor M Eguluz, Raúl Toral, and Maxi San Miguel. Role of dimensionality in axelrod's model for the dissemination of culture. *Physica A: Statistical Mechanics and its Applications*, 327(1-2):1–5, 2003.

[36] Konstantin Klemm, Vıctor M Eguluz, Raul Toral, and Maxi San Miguel. Globalization, polarization and cultural drift. *Journal of Economic Dynamics and Control*, 29(1-2):321–334, 2005.

[37] David J Langley, Tammo HA Bijmolt, J Roland Ortt, and Nico Pals. Determinants of social contagion during new product adoption. *Journal of Product Innovation Management*, 29(4):623–638, 2012.

[38] Natalia Lazzati. Co-diffusion of technologies in social networks. 2017.

[39] Gustave Le Bon. *The crowd*. Routledge, 2017.

[40] Loet Leydesdorff. Technology and culture: The dissemination and the potential'lock-in'of new technologies. *Journal of Artificial Societies and Social Simulation*, 2001.

[41] Daqing Li, Pengju Qin, Huijuan Wang, Chaoran Liu, and Yinan Jiang. Epidemics on interconnected lattices. *EPL (Europhysics Letters)*, 105(6):68004, 2014.

[42] Richard G Lipsey, Kenneth I Carlaw, and Clifford T Bekar. *Economic transformations: general purpose technologies and long-term economic growth*. OUP Oxford, 2005.

[43] Meng Liu, Daqing Li, Pengju Qin, Chaoran Liu, Huijuan Wang, and Feilong Wang. Epidemics in interconnected small-world networks. *PloS one*, 10(3):e0120701, 2015.

[44] Shuangling Luo, Yanyan Du, Peng Liu, Zhaoguo Xuan, and Yanzhang Wang. A study on coevolutionary dynamics of knowledge diffusion and social network structure. *Expert Systems with Applications*, 42(7):3619–3633, 2015.

[45] Robert M May and Martin A Nowak. Coinfection and the evolution of parasite virulence. *Proceedings of the Royal Society of London B: Biological Sciences*, 261(1361):209–215, 1995.

[46] John A Norton and Frank M Bass. A diffusion theory model of adoption and substitution for successive generations of high-technology products. *Management science*, 33(9):1069–1086, 1987.

[47] Martin A Nowak. *Evolutionary dynamics*. Harvard University Press, 2006.

[48] Martin A Nowak and Robert M May. Superinfection and the evolution of parasite virulence. *Proceedings of the Royal Society of London B: Biological Sciences*, 255(1342):81–89, 1994.

[49] Renana Peres, Eitan Muller, and Vijay Mahajan. Innovation diffusion and new product growth models: A critical review and research directions. *International Journal of Research in Marketing*, 27(2):91–106, 2010.

[50] Robert A Peterson and Vijay Mahajan. Multi-product growth models. *Research in marketing*, 1(20):1–23, 1978.

[51] Everett M Rogers. *Diffusion of innovations*. Simon and Schuster, 2010.

[52] Panpan Shu, Lei Gao, Pengcheng Zhao, Wei Wang, and H Eugene Stanley. Social contagions on interdependent lattice networks. *Scientific reports*, 7:44669, 2017.

[53] The Guardian. Don't dismiss bankers' predictions of a bitcoin bubble they should know, Sep 2017.

[54] Michael Trusov, Randolph E Bucklin, and Koen Pauwels. Effects of word-of-mouth versus traditional marketing: findings from an internet social networking site. *Journal of marketing*, 73(5):90–102, 2009.

[55] Thomas W Valente. Network models of the diffusion of innovations. 1995.

[56] Ruud van de Bovenkamp, Fernando Kuipers, and Piet Van Mieghem. Domination-time dynamics in susceptible-infected-susceptible virus competition on networks. *Physical Review E*, 89(4):042818, 2014.

[57] Christophe Van den Bulte and Gary L Lilien. Medical innovation revisited: Social contagion versus marketing effort. *American Journal of Sociology*, 106(5):1409–1435, 2001.

[58] Christophe Van den Bulte and Stefan Stremersch. Social contagion and income heterogeneity in new product diffusion: A meta-analytic test. *Marketing Science*, 23(4):530–544, 2004.

[59] Jian-Xiong Zhang, Qiang Dong Duan-Bing Chen, and Zhi-Dan Zhao. Identifying a set of influential spreaders in complex networks. *Scientific reports*, 6, 2016.